

**Part I**  
**Radioactivity in the Terrestrial**  
**Environment**

# Chapter 1

## Nuclear Magnetic Resonance Study of Cs Adsorption onto Clay Minerals

Yomei Tokuda, Yutaro Norikawa, Hirokazu Masai, Yoshikatsu Ueda, Naoto Nihei, Shigeto Fujimura, and Yuji Ono

**Abstract** The release of radioactive cesium into the environment in the aftermath of disasters such as the Fukushima Daiichi disaster poses a great health risk, particularly since cesium easily spreads in nature. In this context, we perform solid-state nuclear magnetic resonance (NMR) experiments to study Cs<sup>+</sup> ions adsorbed by clay minerals to analyze their local structure. The NMR spectra show two kinds of peaks corresponding to the clays (illite and kaolinite) after immersion in CsCl aqueous solution; the peak at −30 ppm is assigned to Cs<sup>+</sup> on the clay surface while that at −100 ppm is assigned to Cs<sup>+</sup> in the silicate sheet in the clay crystal. This result is consistent with the fact that Cs<sup>+</sup> with smaller coordination number yields a small field shift in the NMR spectra. Moreover, after immersion in KCl aqueous solution, these peaks disappear in the NMR spectra, thereby indicating that our assignment is reasonable. This is because Cs<sup>+</sup> on the clay surface and in the silicate sheet is easily subject to ion exchange by K<sup>+</sup>. We believe that our findings will contribute to a better understanding of the pathway through which Cs transfers from the soil to plants and also to the recovery of the agriculture in Fukushima.

---

Y. Tokuda (✉) • Y. Norikawa • H. Masai  
Institute for Chemical Research, Kyoto University, Gokasho, Uji, Kyoto 611-0011, Japan  
e-mail: [tokuda@noncry.kuicr.kyoto-u.ac.jp](mailto:tokuda@noncry.kuicr.kyoto-u.ac.jp)

Y. Ueda  
Research Institute for Sustainable Humanosphere, Kyoto University, Gokasho, Uji,  
Kyoto 611-0011, Japan

N. Nihei  
Graduate School of Agricultural and Life Sciences, The University of Tokyo, 1-1-1, Yayoi,  
Bunkyo-ku, Tokyo, Japan

S. Fujimura  
NARO Tohoku Agricultural Research Center, 50 Harajukuminami, Arai, Fukushima-shi,  
Fukushima 960-2156, Japan

Y. Ono  
Fukushima Agricultural Technology Centre, 116, Shimonakamichi, Takakura, Hiwadamachi,  
Koriyama, Fukushima 963-0531, Japan

**Keywords** Radioactive cesium • Cs adsorption by soil • Cs NMR spectra  
• Kaolinite • Illite

## 1.1 Introduction

The occurrence of the Tohoku earthquake on March 11, 2011, led to the meltdown of the Fukushima Daiichi Nuclear Power Station in Japan. The accident released several kinds of radioactive elements such as  $^{90}\text{Sr}$ ,  $^{134}\text{Cs}$ ,  $^{137}\text{Cs}$ , and  $^{131}\text{I}$  into the environment. Human exposure to  $^{137}\text{Cs}$  is a health risk because of its long half-life [1]. The element  $^{137}\text{Cs}$  is mostly stabilized in the soil while small quantities are absorbed by plants such as rice [2]. In this manner,  $^{137}\text{Cs}$  seeps into the food chain, leading to its internal exposure in humans and animals. In order to avoid internal exposure, it is important to understand the mechanism underlying its transfer from the soil to plants. Recently, it has been reported that the Cs transfer coefficient exhibits variation even for plants grown in soils with similar levels of radioactivity [3, 4]. Moreover, artificially added  $^{137}\text{Cs}$  can be more easily absorbed by plants than stable Cs in the soil [5]. Thus, we have considered that one of the reasons for this phenomenon is the varied ways in which Cs (i.e., different Cs states) is adsorbed onto clay minerals in the soils.

The clay minerals that stabilize Cs include 1:1-type layer silicates and 2:1-type layer silicates [6]. These silicates stabilize Cs on the surface and silicate sheets because of their negative charges. In particular, in the case of 2:1-type layer silicates, Cs is strongly adsorbed at frayed edge sites (FESs) [7–10]. In this context, it is necessary to understand the stabilization mechanism to analyze the structure of Cs in the clay surface, silicate sheet, and FESs.

The concentration of Cs in the environment is of the order of parts per billion (ppb) or parts per trillion (ppt). Thus, very fine measurement techniques are required to measure such minute quantities and obtain their structural information. The technique of X-ray absorption fine structure (XAFS) spectroscopy is suitable for such measurements [11, 12]. However, the technique of XAFS requires synchrotron radiation, and hence, the method cannot be used in the laboratory. Therefore, another complementary method is required.

In this context, solid-state nuclear magnetic resonance (NMR) has been used to analyze the local structure of Cs in crystals and conventional glasses [13]. As regards the NMR spectra of cesium silicate crystals,  $\text{Cs}^+$  ions with large coordination numbers (CNs) such as  $\text{Cs}_6\text{Si}_{10}\text{O}_{23}$  exhibit a large field shift while those with smaller CNs ( $\text{Cs}_2\text{Si}_2\text{O}_5$ ) exhibit a small field shift. In addition, the same relationship also holds for Cs present in mixed alkali silicate glasses. This relationship can be used to study the local structure of Cs in clay minerals. Moreover, solid-state NMR of clay minerals can be utilized to distinguish Cs on the surface and within silicate sheets [14–17]. In this study, we discuss the structure of Cs adsorbed onto two kinds of clay minerals (kaolinite as 1:1-type layer silicates and illite as 1:2-type layer silicates) by using solid state NMR together with XAFS spectroscopy.

## 1.2 Experimental

### 1.2.1 Sample Preparation

Kaolinite (Wako Chemicals), illite (G-O networks),  $^{133}\text{CsCl}$  (Wako Chemicals), KCl (Wako Chemicals), and ultrapure water (Wako Chemicals) were used as received in our experiments. First, 5 g of illite was immersed in 50 mL of 0.01 M CsCl aqueous solution over time periods of 1 day, 1 month, 6 months, and 2 years. After immersion, the illite samples were separated by centrifugation. Next, 50 mL of ultrapure water was added to each illite sample followed by centrifugal separation. This washing process was performed twice. After washing, the illites were dried overnight at 40 °C. We referred to the various samples as illite\_1d, illite\_1m, illite\_6m, and illite\_2y depending on their immersion periods of 1 day, 1 month, 6 months, and 2 years, respectively. For comparison purposes, kaolinite was also immersed in 50 mL of 0.01 M CsCl aqueous solution over 1 day, 1 month, and 6 months. The kaolinites were also washed using the abovementioned washing process. Following the nomenclature used for the illite samples, we named the kaolinite samples as kaolinite\_1d, kaolinite\_1m, and kaolinite\_6m.

In order to remove the Cs adsorbed onto illite, 1 g of the sample illites\_2y was immersed in 50 mL of 0.01 KCl aqueous solution for 2 h and 2 days. These illites were also washed as per the abovementioned washing process. These “re-ion-exchanged” samples were referred to as illite\_2y\_KCl2h and illite\_2y\_KCl2d.

Further, pristine samples of illite and kaolinite were also analyzed. Table 1.1 lists all the analyzed samples along with the corresponding experimental conditions.

**Table 1.1** Sample notations of clay minerals used in this study

Notation	Period of immersion in CsCl(aq)	Period of immersion in KCl(aq) after immersion in CsCl(aq)
illite_pristine	–	–
illite_1d	1 day	–
illite_6m	6 months	–
illite_2y	2 years	–
illite_2y_KCl2h	2 years	2 h
illite_2y_KCl2d	2 years	2 days
kaolinite_pristine	–	–
kaolinite_1d	1 day	–
kaolinite_6m	6 months	–

### 1.3 Structure Analyses

The crystal structures were analyzed by powder X-ray diffraction (XRD) (RINT 2100, RIGAKU). We used a Cu X-ray source that was operated at 40 kV and 40 mA via the conventional  $2\theta/\theta$  method. The diffractions were acquired at intervals of  $0.02^\circ$ . The extended X-ray absorption fine structure (EXAFS) spectra were obtained at the cesium K-absorption edge via the fluorescence method (BL14B2, SPring-8). The cumulated number of measurements was 40. The XAFS spectra were analyzed by using ATHENA [18].

The solid-state  $^{133}\text{Cs}$  NMR spectra of all the samples were acquired using a Chemagnetics CMX400 spectrometer utilizing a commercial probe (4 mm). The rotation speed was set to 10 kHz with an accuracy  $\pm 10$  Hz. At an external field of 9.4 T, the resonance frequency was set to about 103.7 MHz. For each measurement, the widths of the  $90^\circ$  pulses were set to 2.2  $\mu\text{s}$ . The spectra were obtained with a cycle time of 10 s. The chemical shift reference was 1 mol/L CsCl aqueous solution, whose chemical shifts were set to 0 ppm.

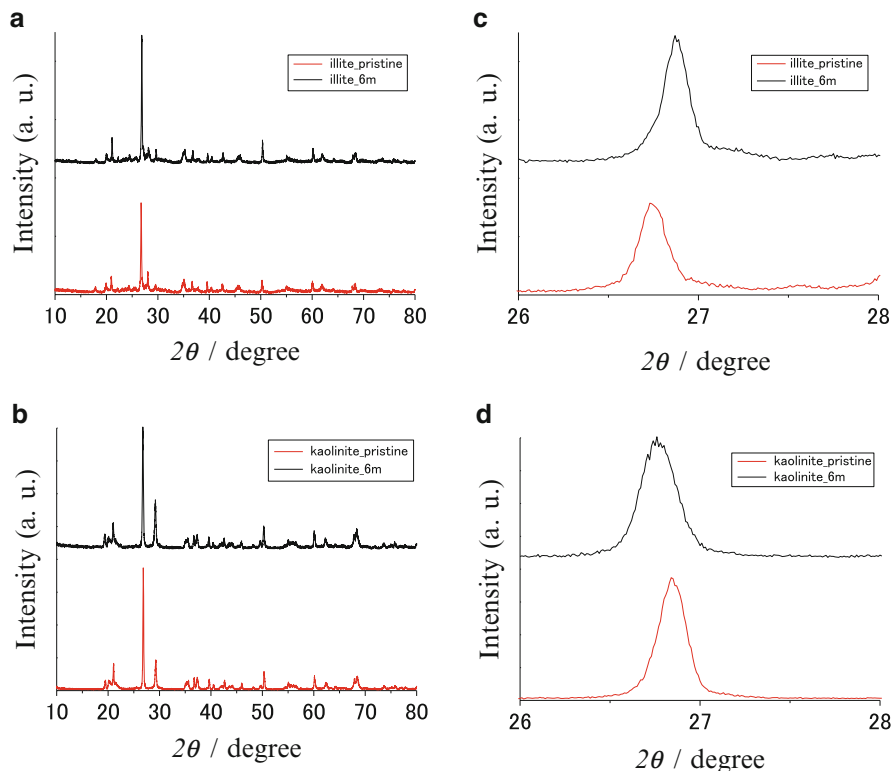
### 1.4 Results

Figure 1.1 shows the XRD patterns of the illite\_pristine, illite\_6m, kaolinite\_pristine, and kaolinite\_6m samples. In the case of illite, the peak around  $27^\circ$  shows a shift to a higher angle after immersion in CsCl, thereby indicating a decrease in the lattice constant. On the other hand, for kaolinite, the peak around  $27^\circ$  shifts to a lower angle, which indicates an increase in the lattice constant.

Figure 1.2 shows  $k^2$ -weighted K-edge EXAFS spectra for the illite\_2y and illite\_2y\_KCl2h samples. As previously reported for the radial distribution functions (RDFs), the first, second, and third peaks can be assigned to Cs–O, Cs–Si, and Cs–Cs, respectively [19, 20]. However, we have not obtained the RDF in the present stage. We can just note that there is a little change in EXAFS spectra for the illite\_2y and illite\_2y\_KCl2h samples.

Figure 1.3 shows the  $^{133}\text{Cs}$  NMR spectra of the illite and kaolinite samples after immersion in CsCl solution. The NMR spectra for all the illites exhibit peaks at around  $-30$  and  $-100$  ppm. On the other hand, the NMR spectra for kaolinite\_1d and \_1m exhibit only one peak at around  $-30$  ppm. The kaolinite\_6m sample (which was immersed for a longer time) exhibits a clear peak at around  $-30$  ppm and a small peak at around  $-100$  ppm.

The effect of re-ion-exchanging by  $\text{K}^+$  on the NMR spectra was also studied (Fig. 1.4). The NMR peak for illite\_2y\_KCl2d vanished, although the peak at around  $-30$  ppm was still observed for illite\_2y\_KCl2h.



**Fig. 1.1** XRD patterns of illite (a) as received and after immersion in KCl solution, (b) kaolinite as received and after immersion in KCl solution. Highest peaks around  $27^\circ$  assigned to (0 0 6) are also shown as (c) and (d)

## 1.5 Discussion

After sample immersion in CsCl solution, the lattice constant change for illite is different from that for kaolinite, as shown in Fig. 1.1; the lattice constant of illite decreases, while that of kaolinite increases. This is because hydrated  $K^+$  in the silicate sheet is replaced by  $Cs^+$  in illite; on the other hand, in the case of kaolinite, a proton is replaced by  $Cs^+$ . Alteration in the  $k^2$ -weighted K-edge EXAFS spectra for illite after immersion in CsCl solution as shown in Fig. 1.2 may support these observations.

As shown in Fig. 1.3, the NMR spectra of illite exhibit two peaks at  $-30$  and  $-100$  ppm, while those of kaolinite exhibit two peaks (one clear peak and one very small peak at  $-30$  and  $-100$  ppm, respectively). Kaolinite has a negative surface charge on the crystallite. Accordingly, the clear peak at  $-30$  ppm can be assigned to the surface  $Cs^+$ . In contrast, illite has a negative charge between silicate sheets. As a result, the peaks at  $-100$  ppm can be assigned to  $Cs^+$  in the silicate sheets.

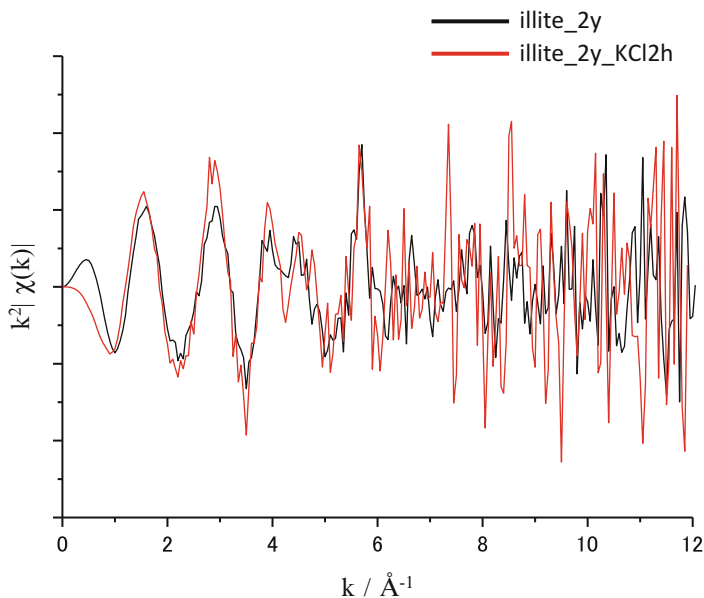


**Fig. 1.2**  $k^2$ -weighted K-edge EXAFS spectra for illite\_2y and illite\_2y\_KCl2h

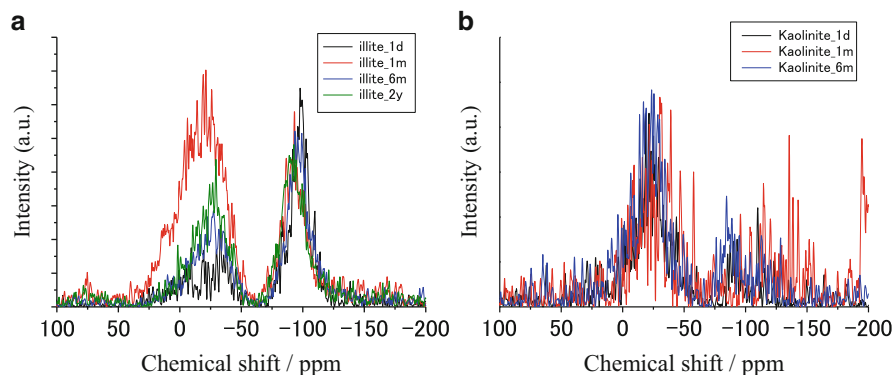


**Fig. 1.3** NMR spectra of clays immersed in CsCl aqueous solution for several periods (a) illite, (b) kaolinite. The chemical shift reference is CsCl (aq)

These assignments agree well with the results of previous NMR experiments;  $\text{Cs}^+$  with larger CN values exhibits a large field shift, while that with smaller CN values exhibits a small field shift [13]. In another NMR experiment, there also existed two kinds of peaks for illite immersed in CsCl [14]. These results also support our assignment.

After re-ion-exchange (using KCl) over a relatively long period (2 days) for illite (Fig. 1.4), no peak was observed in the NMR spectrum, thereby indicating that all

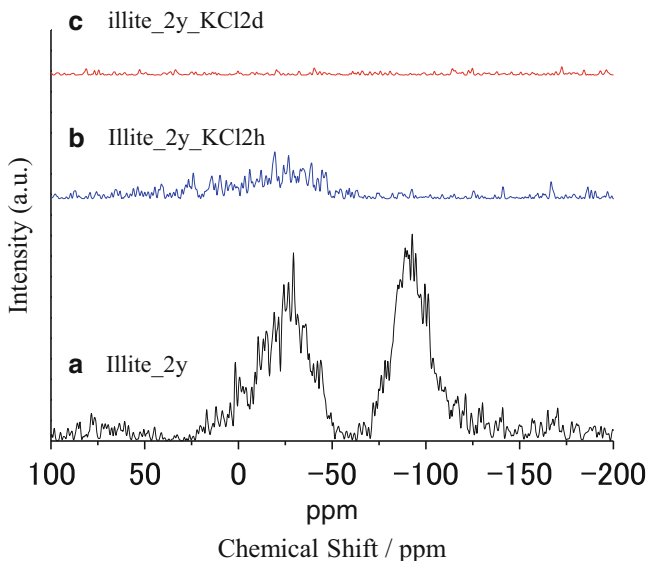


**Fig. 1.4** NMR spectra of illite (a) immersion in CsCl solution for 2 years, (b) ion-exchanged illite by immersion in KCl for 2 h, (c) ion-exchanged illite by immersion in KCl for 2 days. The chemical shift reference is CsCl (aq)

the  $\text{Cs}^+$  ions on the surface and in the silicate sheet had been replaced by  $\text{K}^+$ . This result supports our assignment because  $\text{Cs}^+$  on the clay surface and in the silicate sheet is easily ion-exchanged by  $\text{K}^+$  [6]. This result also indicates that no FESs were observed in this experiment. One of the reasons for the absence of the FES signature is the low concentration of the total amount of  $\text{Cs}^+$ . After re-ion-exchange for a short period of time (2 h), we observed only one peak at  $-30$  ppm. This result can be attributed to the fact that  $\text{Cs}^+$  in the silicate sheet is more easily replaced by  $\text{K}^+$  than that on the surface.

In conclusion, solid-state  $^{133}\text{Cs}$  NMR is useful for analyzing  $\text{Cs}^+$  adsorbed onto clay minerals; this method can be used to distinguish  $\text{Cs}^+$  sites in the clay minerals. In the near future, we plan to perform structure analysis of  $\text{Cs}^+$  in soil in order to understand the mechanism of transfer of Cs from the soil to plants. We believe that this study will contribute to the recovery of agriculture in Fukushima in the near future.

## 1.6 Conclusions

We performed  $^{133}\text{Cs}$  NMR experiments in conjunction with XRD and EXAFS to analyze the adsorption of  $\text{Cs}^+$  onto clay minerals such as illite and kaolinite. Our NMR results indicate that the observed peaks at  $-30$  and  $-100$  ppm can be assigned



to Cs<sup>+</sup> on the surface and in the silicate sheet, respectively. After re-ion-exchange by using aqueous KCl, the Cs<sup>+</sup> ions were replaced by K<sup>+</sup> ions. We believe that our findings will contribute to a better understanding of the mechanism of Cs transfers from the soil to plants. We plan to use the NMR method in our future studies on understanding of the mechanism of transfer of Cs<sup>+</sup> from the soil to plants.

**Acknowledgments** This work was supported by the Collaborative Research Program of Institute for Chemical Research, Kyoto University (No. 2015- 68, 70), Research Institute for Sustainable Humanosphere, Kyoto University, and Kureha Trading Co., Ltd. The synchrotron radiation experiments were performed at the BL14B2 beamline of the SPring-8 facility with the approval of the Japan Synchrotron Radiation Research Institute (JASRI) (Proposal No. 2015A1662). We would like to thank Kenji Hara, Hiroshi Goto and Hironori OFuchi for fruitful discussions.

**Open Access** This chapter is distributed under the terms of the Creative Commons Attribution Noncommercial License, which permits any noncommercial use, distribution, and reproduction in any medium, provided the original author(s) and source are credited.

## References

1. IAEA (2006) Environmental consequences of the Chernobyl accident and their remediation: twenty years of experience. International Atomic Energy Agency, Vienna
2. Fujimura S, Muramatsu Y, Ohno T, Saitou M, Suzuki Y, Kobayashi T, Yoshioka K, Ueda Y (2015) Accumulation of (137)Cs by rice grown in four types of soil contaminated by the Fukushima Dai-ichi Nuclear Power Plant accident in 2011 and 2012. *J Environ Radioact* 140:59–64
3. Kato N, Kihou N, Fujimura S, Ikeba M, Miyazaki N, Saito Y, Eguchi T, Itoh S (2015) Potassium fertilizer and other materials as countermeasures to reduce radiocesium levels in rice: results of urgent experiments in 2011 responding to the Fukushima Daiichi Nuclear Power Plant accident. *Soil Sci Plant Nutr* 61:179–190
4. Ehlfen S, Kirchner G (2002) Environmental processes affecting plant root uptake of radioactive trace elements and variability of transfer factor data: a review. *J Environ Radioact* 58:97–112
5. Tsukada H, Nakamura Y (1999) Transfer of <sup>137</sup>Cs and stable Cs from soil to potato in agricultural fields. *Sci Total Environ* 228:111–120
6. Yamaguchi N, Takata Y, Hayashi K, Ishikawa S, Kuramata M, Eguchi S, Yoshikawa S, Sakaguchi A, Asada K, Wagai R, Makino T, Akahane I, Hiradate S (2012) Behavior of radiocesium in soil-plant systems and its controlling factor (in Japanese). *Bull Nat Inst Agro-Environ Sci* 31:75–129
7. Fuller AJ, Shaw S, Ward MB, Haigh SJ, Mosselmans JFW, Peacock CL, Stackhouse S, Dent AJ, Trivedi D, Burke IT (2015) Caesium incorporation and retention in illite interlayers. *Appl Clay Sci* 108:128–134
8. Okumura M, Nakamura H, Machida M (2014) First-principles studies of cesium adsorption to frayed edge sites of micaceous clay minerals. In: Abstract paper of the [248thAmericanchemicalsocietynationalmeeting&exposition](#), San Francisco
9. Sato K, Fujimoto K, Dai W, Hunger M (2013) Molecular mechanism of heavily adhesive Cs: why radioactive Cs is not decontaminated from soil. *J Phys Chem C* 117:14075–14080
10. Cremers A, Elsen A, Depreter P, Maes A (1988) Quantitative-analysis of radiocesium retention in soils. *Nature* 335:247–249

11. Fan Q, Yamaguchi N, Tanaka M, Tsukada H, Takahashi Y (2014) Relationship between the adsorption species of cesium and radiocesium interception potential in soils and minerals: an EXAFS study. *J Environ Radioact* 138:92–100
12. Bostick BC, Vairavamurthy MA, Karthikeyan KG, Chorover J (2002) Cesium adsorption on clay minerals: an EXAFS spectroscopic investigation. *Environ Sci Technol* 36:2670–2676
13. Minami T, Tokuda Y, Masai H, Ueda Y, Ono Y, Fujimura S, Yoko T (2014) Structural analysis of alkali cations in mixed alkali silicate glasses by  $^{23}\text{Na}$  and  $^{133}\text{Cs}$  MAS NMR. *J Asian Ceram Soc* 2:333–338
14. Kim Y, Cygan RT, Kirkpatrick RJ (1996)  $^{133}\text{Cs}$  NMR and XPS investigation of cesium adsorbed on clay minerals and related phases. *Geochim Cosmochim Acta* 60:1041–1052
15. Kim Y, Kirkpatrick RJ (1997)  $^{23}\text{Na}$  and  $^{133}\text{Cs}$  NMR study of cation adsorption on mineral surfaces: local environments, dynamics, and effects of mixed cations. *Geochim Cosmochim Acta* 61:5199–5208
16. Kim Y, Kirkpatrick RJ, Cygan RT (1996)  $^{133}\text{Cs}$  NMR study of cesium on the surfaces of kaolinite and illite. *Geochim Cosmochim Acta* 60:4059–4074
17. Maekawa A, Momoshima N, Sugihara S, Ohzawa R, Nakama A (2014) Analysis of  $^{134}\text{Cs}$  and  $^{137}\text{Cs}$  distribution in soil of Fukushima prefecture and their specific adsorption on clay minerals. *J Radioanal Nucl Chem* 303:1485–1489
18. Ravel B, Newville M (2005) ATHENA, ARTEMIS, HEPHAESTUS: data analysis for X-ray absorption spectroscopy using IFEFFIT. *J Synchrotron Radiat* 12:537–541
19. Yaita T (2013) Interpretation of Cs adsorption behavior based on the EXAFS, TR-Dxafs, and STXM methods. *Mineral Mag* 77:2532
20. Yaita T, McKinley I (2013) Fundamental approaches toward development of radiocesium removal methods from soil and the other related materials, waste reduction and management optimization. [http://fukushima.jaea.go.jp/initiatives/cat01/pdf00/07\\_\\_Yaita.pdf](http://fukushima.jaea.go.jp/initiatives/cat01/pdf00/07__Yaita.pdf)

## Chapter 2

# Speciation of $^{137}\text{Cs}$ and $^{129}\text{I}$ in Soil After the Fukushima NPP Accident

Tomoko Ohta, Yasunori Mahara, Satoshi Fukutani, Takumi Kubota, Hiroyuki Matsuzaki, Yuji Shibahara, Toshifumi Igarashi, Ryoko Fujiyoshi, Naoko Watanabe, and Tamotsu Kozaki

**Abstract** We evaluated the migration of radionuclides ( $^{131}\text{I}$ ,  $^{129}\text{I}$ ,  $^{134}\text{Cs}$ ,  $^{136}\text{Cs}$ ,  $^{137}\text{Cs}$ , and  $^{132}\text{Te}$ ) in the surface soil after the Fukushima nuclear accident. The radionuclides in the soil collected late March in 2011 were barely leached with ultrapure water, indicating that these are insoluble. We observed the chemical behavior of  $^{137}\text{Cs}$  and  $^{129}\text{I}$  in soil: (1)  $^{137}\text{Cs}$  was predominantly adsorbed within a depth of 2.5 cm from the ground surface; (2)  $^{137}\text{Cs}$  was hardly released from soil by the water leaching experiments that lasted for 270 days; (3) approximately, more than 90 % of  $^{137}\text{Cs}$  was adsorbed on organic matters and the residual fractions, while  $^{129}\text{I}$  was mainly fixed on the Fe-Mn oxide and organically bounded fraction. Therefore, we conclude that  $^{137}\text{Cs}$  and  $^{129}\text{I}$  in soil seldom leach into the soil water and migrate downward because of the irreversible adsorption. The shallow groundwater which residence time is short.

**Keywords** Cesium-137 • Iodine-129 • Speciation • Soil • Fukushima nuclear accident • Migration • Groundwater

---

T. Ohta (✉) • T. Igarashi • R. Fujiyoshi • N. Watanabe • T. Kozaki  
Faculty of Engineering, Hokkaido University, Nishi8, Kita13, Sapporo, Hokkaido 060-8628,  
Japan  
e-mail: [tomohta@eng.hokudai.ac.jp](mailto:tomohta@eng.hokudai.ac.jp)

Y. Mahara  
Kyoto University, Yosidahonmachi, Sakyoku-ku, Kyoto-Shi, Kyoto 606-8501, Japan  
The University Museum, The University of Tokyo, 16, 11, 2, Yayoi, Bunkyo-ku,  
Tokyo 113-0032, Japan

H. Matsuzaki  
The University Museum, The University of Tokyo, 16, 11, 2, Yayoi, Bunkyo-ku,  
Tokyo 113-0032, Japan

S. Fukutani • T. Kubota • Y. Shibahara  
Research Reactor Institute, Kyoto University, Kumatori, Sennangun, Osaka 590-0494, Japan

## 2.1 Introduction

A number of radionuclides (including  $^{137}\text{Cs}$ ,  $^{134}\text{Cs}$ ,  $^{136}\text{Cs}$ ,  $^{131}\text{I}$ ,  $^{132}\text{Te}$ ) were released into the atmosphere from the Fukushima Daiichi NPP accident in March, 2011. On March 15–17 and 21–23, deposition increased in the areas surrounding Fukushima prefecture because north–easterly, easterly, and south–easterly winds under a low-pressure system transported the radionuclides from the Fukushima NPP, and subsequent precipitation associated with the same system washed radioactive materials out of the radioactivity plume, thereby effectively depositing them on land [1–5]. In addition to the radioactive plume that covered the Fukushima Prefecture, two other large plumes suffered severe radioactive contamination over north Japan. Precipitation from these plumes caused high-radioactive spots across wide areas including the Tokyo metropolitan [1].

Although the eastern parts in the Tokyo metropolitan area are located far from the Fukushima NPP, high  $^{137}\text{Cs}$  and  $^{131}\text{I}$  deposition was observed in the areas. Therefore, the Tokyo metropolitan area is one of the hot spots of radioactive fallout from the Fukushima NPP accident [4]. The Tokyo metropolitan hot-spot area has a high-density population, and many residents have been worried about the radiation exposure from the Fukushima NPP. The released  $^{131}\text{I}$  from the Fukushima NPP contaminated tap water with rainfall that precipitated in the Tokyo metropolitan hot-spot areas on March 23, 2011, whereas  $^{131}\text{I}$  was also detected in the tap water of the Kanto and Tohoku regions through mid-April [1].

At present,  $^{131}\text{I}$  released from the Fukushima NPP accident in March, 2011 is not detected in the environment, because its short half-life is only 8 days. On the contrary,  $^{129}\text{I}$  with a half-life of 15.7 Ma is easily found. The  $^{129}\text{I}/^{127}\text{I}$  ratio measured in surface soil could provide information on the local deposition of  $^{131}\text{I}$  released from the Fukushima NPP, if the ratio of  $^{131}\text{I}$  and  $^{129}\text{I}$  before release from the broken reactors can be estimated [6, 7]. The  $^{131}\text{I}$  behavior in the unsaturated zone and shallow groundwater immediately after the accident may be inferred from the  $^{129}\text{I}$  content.

This study has two objectives: (1) to examine the behavior of  $^{137}\text{Cs}$  and  $^{131}\text{I}$  in the surface soil of the Kanto loam in the Tokyo metropolitan hot-spot areas and Fukushima immediately after the accident and (2) to determine the  $^{137}\text{Cs}$  and  $^{129}\text{I}$  speciation in the soil to evaluate  $^{137}\text{Cs}$  and  $^{131}\text{I}$  contamination in the shallow groundwater which residence time is short.

## 2.2 Material and Methods

### 2.2.1 Soil Samples

One surface-soil sample within a depth of 0.5 cm and four surface-soil samples within a depth of 1 cm were collected on March 29, 2011 at the western Tokyo metropolitan area (WTMA, W1) and on March, 30 and 31, 2011 at the eastern Tokyo

metropolitan hot-spot area (ETMA, E1-4), respectively. The soil samples collected at western Tokyo were placed in a polypropylene vessel (vessel A), 5 cm in diameter and 10 cm in height, and each of the four soil samples collected at eastern Tokyo was packed into a polypropylene vessel (vessel B), 2.2 cm in diameter and 1.2 cm in height.

Surface-soil core samples ( $5\text{ cm}^2 \times 10\text{ cm}$ ) were collected at the WTMA on August 25, 2011 and ETMA, on October 14–18, 2011, respectively. The undisturbed soil cores were sampled using a cylindrical stainless steel core sampler, 0–10 cm in depth. The soil core samples were cut into the lengths of 0–2.5, 2.5–5 cm, and 5–10 or 0–2.5 and 2.5–5.0 cm. Each sample was stored in plastic vessels (vessels A). We also collected soil in the same manner in Nagadoro, Fukushima (N1) in May, 2012. Then we measured the vertical profiles of  $^{137}\text{Cs}$  in soil.

### ***2.2.2 Column-Infiltration Experiments Using the Rainwater from the Tokyo Metropolitan Hot-Spot Area***

It rained in the southern Ibaraki Prefecture from 0:00 to 2:00 LT on March 31, 2011, resulting in a total precipitation of 5.5 mm in Tsukuba. A rainwater sample was collected during precipitation at the ETMA (Japan Meteorological Agency). The rainwater sample (101 mL) was placed in a polypropylene vessel (5 cm in diameter and 10 cm in height, vessel A).

We investigated the infiltration of  $^{137}\text{Cs}$  from the rainwater in the soil environment via column experiments on April 1, 2011. Sand (Toyoura Standard Sand, Toyoura Keiseki Kogyo Co., Ltd., Yamaguchi, Japan) and soil were used in the columns. The soil, classified by the *World Reference Base* as a haplic stagnosol, was collected from a depth of approximately 30 cm from an outcrop at the campus of Kyoto University Research Reactor Institute (KURRI), Osaka, Japan. The soil contained a small amount of organic matter (organic carbon 2.7–2.8 %, pH 5.7–5.8) and was devoid of  $^{137}\text{Cs}$  and  $^{134}\text{Cs}$ .

The sand was rinsed several times to remove clay minerals using deep groundwater that did not contain  $^{137}\text{Cs}$ . The sand and soil samples were packed into two columns (20 mm in diameter and approximately 1 cm in depth). After filling, columns A (sand) and B (soil) were soaked in pure water for 3 h. Next, the rainwater sample (50 mL) was passed through each column at a rate of  $0.7\text{ mL}\cdot\text{min}^{-1}$ , and then, each column was rinsed with ultrapure water (84 mL). Although the flow rate used was faster than the actual rate of rainwater infiltration in the Kanto district (approximately  $1.5\text{ m}\cdot\text{y}^{-1}$ ), this provides a conservative estimation of radionuclide migration. After infiltration, the sand and soil samples were stored separately in polypropylene containers (vessel B). Then, these vessels were placed into a different container, and the radioactivity of the samples in each container was measured using a gamma-ray spectrometer.

**Table 2.1** Concentrations of major ions in groundwater

Element	Concentration (mg·L <sup>-1</sup> )	Element	Concentration (mg·L <sup>-1</sup> )
Na	6.92	Cl <sup>-</sup>	5.83
K	7.00	SO <sub>4</sub> <sup>2-</sup>	13.4
Ca	22.0	HCO <sub>3</sub> <sup>-</sup>	110
Mg	7.87	pH	8.3

### 2.2.3 Leaching of Radionuclides from Soils Using the Batch Method

Radioactivities of the 100-g soil samples collected on March 29, 2011 at WTMA were immediately measured by the following method. The soil samples were mixed with the ultrapure water and shaken by hand for 30 min. The mixture was stored for 15 min, and the solution was separated by ultra-centrifuge (Kokusan Co., Ltd, Japan), and then, radioactivity in the supernatant was measured by gamma-ray spectrometry.

Approximately 10 g of the surface-soil samples collected from the WETA were added to ultrapure and groundwater samples, and then, they were agitated at a speed of 100 rpm for 90 and 270 days. The groundwater sample was discharged from the Kanto-loam layer in the Tokyo metropolitan hot-spot area, and was sampled in March, 2010 before the Fukushima NPP accident. The concentrations of Na<sup>+</sup>, K<sup>+</sup>, Mg<sup>2+</sup>, and Ca<sup>2+</sup> in the groundwater were measured by cation chromatography and those of Cl<sup>-</sup>, SO<sub>4</sub><sup>2-</sup> and NO<sub>3</sub><sup>-</sup> were measured by anion chromatography, whereas HCO<sub>3</sub><sup>-</sup> was measured by titration using HCl. Table 2.1 lists the major cation and anion of the groundwater samples.

After leaching, solid-liquid separation was conducted by centrifugation at 2000 rpm for 5 min. Then, the solution was filtered through a membrane filter with a pore size of 0.45 μm (Advantech, Co., Ltd., Japan). After storing each fraction in a U-8 vessel, radioactivities of <sup>131</sup>I, <sup>134</sup>Cs, <sup>136</sup>Cs, <sup>137</sup>Cs, and <sup>132</sup>Te were measured by gamma-ray spectrometry.

### 2.2.4 Separation of <sup>137</sup>Cs and <sup>129</sup>I in Soil Samples

We extracted <sup>137</sup>Cs and <sup>129</sup>I from three surface soil samples from the Kanto-loam layer in the ETMA and the Nagadoro in Fukushima. The soil of depths of 0–2.5 cm (E5, E6, N1) was well mixed and approximately 10 g soil sample was taken by cone and quartering method. Approximately 10 g of the samples were used in the sequential-extraction experiment [8, 9]. A ratio of solution to sample of 5 (v/w) was used for extraction in each step.

Fraction 1: After ultrapure water was added to the soil sample, the suspension was shaken for 24 h at room temperature, and then the suspension was stored overnight. After extraction, solution was separated from the soil residue by centrifugation at 2000 rpm for 5 min. The solution was filtered through a membrane filter with a pore size of 0.45  $\mu\text{m}$  (Advantech, Co., Ltd., Japan). The fraction of the filtrate represents water-soluble species. The remaining solid on the membrane filter was combined with the residue for the next leaching step.

Fraction 2: 1 M of NaAc was added to the residue from Fraction 1. The suspension was shaken for 12 h at room temperature and stored overnight. The fraction of the filtrate represents exchangeable species.

Fraction 3: 1-M NaAc – HAc (pH 5) was added to the residue from Fraction 2, and the suspension was shaken for 12 h at room temperature. The fraction of the filtrate represents carbonate-bound species.

Fraction 4: 0.04-M  $\text{NH}_2\text{OH}\cdot\text{HCl}$  in 25 % (v/v) HAc (pH 2) was added to the residue from Fraction 3 and stirred in a hot-water bath at 80  $^\circ\text{C}$  for 4 h. The fraction of the filtrate represents species associated with solids via chemical-sorption mechanisms that can be released into the extraction solution with a weak reducing agent, and they mainly include species bound to Fe/Mn oxides.

Fraction 5: 30 %  $\text{H}_2\text{O}_2$  was added to the residue, in which  $\text{HNO}_3$  had already been added to adjust the final pH to 2. The suspension was agitated for 2 h at 85  $^\circ\text{C}$ . After the suspension was cooled to room temperature, 1.8-M  $\text{NH}_4\text{Ac}$  in 11 %  $\text{HNO}_3$  (v/v) was added, and the extraction continued for 30 min at room temperature. The fraction of the filtrate is associated with organic matter.

After each fraction was stored into a U-8 vessel,  $^{137}\text{Cs}$  was measured by gamma-ray spectrometry.

### ***2.2.5 Purification of Iodine Isotopes for Accelerator Mass Spectrometry (AMS) Measurement***

One-milliliter solution of nitric acid (Kanto Chemical Co., Ltd.) and 0.5 mL of  $\text{H}_2\text{O}_2$  (Kanto Chemical Co., Ltd.) were added to sample solutions separated from each fraction. The dissolved iodine was oxidized to  $\text{I}_2$  and was then separated from the sample solution into 10 mL of chloroform (Wako Co., Ltd.). The chloroform was separated from the sample solution, and then 10 mL of 0.1 M of  $\text{NaHSO}_3$  (Wako Co., Ltd.) was added to the chloroform to extract  $\text{I}^-$  into the  $\text{NaHSO}_3$  solution. The  $\text{NaHSO}_3$  solution was separated from the chloroform, and 1 mL of 6 M NaCl (Aldrich Co., Ltd.) was added to the solution. A 0.1 mL portion of 1 M  $\text{AgNO}_3$  (Aldrich Co., Ltd.) was then added to the solution, and the solution was agitated, causing AgI to precipitate with AgCl. This precipitation was allowed to continue for 30 min before the mixture was centrifuged for 5 min at 3000 rpm. The mixture of AgCl and AgI precipitate was separated from the solution. AgCl was separated from AgI by adding 4 mL of concentrated  $\text{NH}_3$  to dissolve AgCl only. The AgI

precipitate was rinsed with 5 mL of ultrapure water to yield a pure AgI sample, which was then dried in an electric oven at 70 °C for 40 min. The AgI sample was added to Nb powder at an Nb and AgI ratio of 4 (w/w). The detail chemical separation was described by a previous paper [10].  $^{129}\text{I}$  and  $^{127}\text{I}$  were measured by AMS (Malt, Tokyo Univ., Japan), and detailed procedure of measurement of  $^{129}\text{I}/^{127}\text{I}$  atomic ratios were described by Matsuzaki et al. [11].

### 2.2.6 Measurement of Radioactivity in Environmental Samples by Gamma-Ray Spectrometry

The radioactivity of the rainwater and soil sample was measured using a p-type high-purity germanium detector (IGC-309, Princeton Gamma-Tech) with 40 % relative efficiency and a multichannel analyzer (7600-000, Seiko EG&G) with a high-voltage circuit (7600-310) and pulse height analyzer (7600-510) in KURRI. The gamma-ray counting efficiency of the detector was estimated by constructing a relative gamma-ray-counting-efficiency curve using a certified mixed-radionuclide gamma-ray reference source containing  $^{57}\text{Co}$  (122.1 keV),  $^{137}\text{Cs}$  (661.7 keV), and  $^{60}\text{Co}$  (1173 and 1332 keV), which were normalized to the 1460-keV gamma-ray peak of  $^{40}\text{K}$  in KCl. A quadratic function was fitted to the logarithmic relationship between the relative counting efficiency and gamma-ray energy using the least-squares method and was normalized at 1460 keV. The radiation energies of  $^{131}\text{I}$ ,  $^{134}\text{Cs}$ ,  $^{136}\text{Cs}$ ,  $^{137}\text{Cs}$ , and  $^{132}\text{Te}$  were 364, 796, 818, 662, and 228 keV, respectively. The sum effect of gamma rays from  $^{134}\text{Cs}$  was corrected by measuring the  $^{134}\text{Cs}$  solution.  $^{134}\text{Cs}$  was produced by the neutron activation of CsCl at KURRI. CsCl was dissolved in the ultrapure water and the prepared  $^{134}\text{Cs}$  solution. The detection limits of  $^{131}\text{I}$ ,  $^{134}\text{Cs}$ , and  $^{137}\text{Cs}$  with a measuring time of 10,000 s were 0.11, 0.099, and 0.12 Bq for vessel B and 0.20, 0.19, and 0.23 Bq for vessel A, respectively.

The radioactivity of undisturbed core samples from the ETMA and radio-Cs samples leaching into the ultrapure water and groundwater samples was measured in the Isotopes Centre, Hokkaido University using a p-type, high-purity germanium detector (model IGC-309, Princeton Gamma-Tech) with 40 % relative efficiency. The detection limits of  $^{134}\text{Cs}$  and  $^{137}\text{Cs}$  with a measuring time of 864,000 s were 0.02 and 0.02 Bq for the U-8 vessel, respectively.

## 2.3 Results and Discussion

Table 2.2 shows the concentrations of  $^{134}\text{Cs}$ ,  $^{136}\text{Cs}$ ,  $^{137}\text{Cs}$ ,  $^{131}\text{I}$ , and  $^{132}\text{Te}$  in the surface soils collected in March, 2011 from the Tokyo metropolitan hot-spot area (but only W6 was collected in August, 2011). Short half-lives for  $^{136}\text{Cs}$ ,  $^{131}\text{I}$ , and  $^{132}\text{Te}$  were detected in the surface-soil samples except W6. The radioactivities of



**Table 2.2** Concentrations of  $^{134}\text{Cs}$ ,  $^{136}\text{Cs}$ ,  $^{137}\text{Cs}$ ,  $^{131}\text{I}$ , and  $^{132}\text{Te}$  in surface soils in Tokyo metropolitan area

Sampling site number	Sampling sites	Depth	Sampling date	$^{134}\text{Cs}$	$^{137}\text{Cs}$
		cm		$\text{kBq}\cdot\text{kg}^{-1}$	$\text{kBq}\cdot\text{kg}^{-1}$
W1	WTMA	0–0.5	March 29, 2011	$0.517 \pm 0.01$	$0.530 \pm 0.07$
E1	ETMA	0–1	March 30, 2011	$2.86 \pm 0.07$	$3.25 \pm 0.07$
E2	ETMA	0–1	March 30, 2011	$2.70 \pm 0.14$	$2.90 \pm 0.12$
E3	ETMA	0–1	March 31, 2011	$1.01 \pm 0.06$	$0.720 \pm 0.06$
E4	ETMA	0–1	March 31, 2011	$1.80 \pm 0.07$	$1.70 \pm 0.18$
W6	WTMA	0–5	Aug. 25, 2011	$0.078 \pm 0.002$	$0.093 \pm 0.002$
		$^{131}\text{I}$	$^{136}\text{Cs}$	$^{132}\text{Te}$	$^{134}\text{Cs}/^{137}\text{Cs}$
		$\text{kBq}\cdot\text{kg}^{-1}$	$\text{kBq}\cdot\text{kg}^{-1}$	$\text{kBq}\cdot\text{kg}^{-1}$	
W1	WTMA	$3.43 \pm 0.01^a$	$0.051 \pm 0.002^a$	$0.373 \pm 0.05^a$	$1.03 \pm 0.13$
E1	ETMA	$9.36 \pm 0.10^b$	$0.301 \pm 0.360^b$	$0.338 \pm 0.050^b$	$1.14 \pm 0.03$
E2	ETMA	$11.1 \pm 0.21^b$	$0.220 \pm 0.056^b$	$0.168 \pm 0.074^b$	$1.07 \pm 0.07$
E3	ETMA	$13.4 \pm 0.2^b$	$0.128 \pm 0.050^b$	$0.271 \pm 0.056^b$	$0.71 \pm 0.10$
E4	ETMA	$7.32 \pm 0.12^b$	$0.632 \pm 0.076^b$	$0.328 \pm 0.049^b$	$0.94 \pm 0.11$
W6	WTMA	–	–	–	$1.19 \pm 0.03$

WTMA Western Tokyo metropolitan area, ETMA Eastern Tokyo metropolitan area

<sup>a</sup>Correction at 5:00 March 29, 2011 at local time

<sup>b</sup>Correction at 2:00 March 31, 2011 at local time

$^{131}\text{I}$ ,  $^{134}\text{Cs}$ , and  $^{137}\text{Cs}$  in the surface-soil samples except W6 collected at ETMA were measured, and W6 measured only the radioactivities of  $^{134}\text{Cs}$  and  $^{137}\text{Cs}$ .  $^{131}\text{I}$  was the source of the maximum radioactivity in the soil in March, 2011 in the Tokyo metropolitan hot-spot area. The concentration of  $^{131}\text{I}$  ranged from 9.4 to 13  $\text{k Bq}\cdot\text{kg}^{-1}$  before rain (March 30, 2011) and from 7.2 to 11  $\text{k Bq}\cdot\text{kg}^{-1}$  after rain, whereas that of  $^{137}\text{Cs}$  ranged from 0.72 to 3.3  $\text{k Bq}\cdot\text{kg}^{-1}$  before rain and 1.7–2.9  $\text{k Bq}\cdot\text{kg}^{-1}$  after rain (March 31). As the fallout radionuclides on the surface soils were mainly washed out from the atmospheric aerosol plume by precipitation,  $^{137}\text{Cs}$  concentrations being similar to  $^{131}\text{I}$  in the soil before rain on March 30 and after rain on March 31 suggest that the rainfall on March 21 and 22 (and the very small precipitation on March 15 and 16) was major source to most radionuclides in the soil.

The concentrations of  $^{131}\text{I}$ ,  $^{134}\text{Cs}$ , and  $^{137}\text{Cs}$  in the rainwater collected at the ETMA toward the end of March, 2011 were  $66 \pm 3$ ,  $28 \pm 2$ , and  $31 \pm 2 \text{ Bq}\cdot\text{L}^{-1}$ , respectively. The concentration of each radionuclide was corrected at 2:00 LT, 31 March 2011.

**Table 2.3** Radioactivities collected in sand and soil (column A and B), and collection efficiencies

Sample ID	Sand column	Soil column
Material	Sand	Soil
Weight (g)	3.2	4.7
<sup>131</sup> I (Bq)	ND	0.82 ± 0.06
<sup>137</sup> Cs (Bq)	1.44 ± 0.09	1.26 ± 0.08
<sup>131</sup> I collection efficiency (%)	–	31 ± 3
<sup>137</sup> Cs collection efficiency (%)	93 ± 6	81 ± 5

ND: below detection limit

Table 2.3 lists radioactivities trapped in both columns of sand and soil, and the <sup>131</sup>I- and <sup>137</sup>Cs-trapping efficiencies in both columns. In column A (sand), almost all of the <sup>137</sup>Cs was trapped on sand with the trapping efficiency of 93 ± 6 %. In column B (soil), the <sup>137</sup>Cs-trapping efficiency was 81 ± 5 %. Therefore, we considered almost all <sup>137</sup>Cs in rainwater to be adsorbed on sand and the Haplic Gray Upland soil within a depth of 1 cm from the ground, while the trapping efficiency of <sup>131</sup>I in both sand and soil columns was below the detection limit and 30 %, respectively. These data indicate that retardation of <sup>131</sup>I in both sand and soil downward was smaller than that of <sup>137</sup>Cs.

Table 2.4 shows the concentrations of <sup>137</sup>Cs and <sup>134</sup>Cs in the surface soil collected at the ETMA in October, 2011, 7 months after the accident. Almost all <sup>134</sup>Cs and <sup>137</sup>Cs in the Kanto-loam soil were within a depth of 2.5 cm from the ground. The column test and the distribution of <sup>137</sup>Cs obtained from the core sample in the field indicated that <sup>134</sup>Cs and <sup>137</sup>Cs were strongly adsorbed on the surface soil within a depth of several centimetres from the surface. Vertical profiles of radionuclides in soil in Koriyama, Fukushima, showed that more than 90 % of <sup>131</sup>I was found to be within about 5 cm depth from the surface in soil layer after the accident [12].

Following the leaching tests from the surface soil collected at WTMA into the pure water immediately after sampling in March, 2011, the leachate was separated from soil. <sup>134</sup>Cs, <sup>137</sup>Cs, <sup>131</sup>I, <sup>136</sup>Cs, and <sup>132</sup>Te in soil did not leach into the water (Table 2.5). Table 2.5 lists the amount of radioactive Cs in the leachate when the surface soil of the ETMA or WTMA was mixed with the ultrapure water and groundwater during 90 and 270 days. Both <sup>137</sup>Cs and <sup>134</sup>Cs in each soil of the Kanto-loam layer and the Nagadoro were not released by leaching with both the ultrapure water and groundwater after mixing during 90 and 270 days.

Table 2.6 shows the leaching fractions of <sup>137</sup>Cs from each soil in the Kanto-loam layer of the ETMA and in the Nagadoro, Fukushima according to the sequential-extraction procedure described previously. The amount of <sup>137</sup>Cs leached into water (F1) from the Kanto-loam soil and Fukushima soil was below the detection limit. This has been demonstrated by the leaching results of radioactive Cs from the soil by the ultrapure water and groundwater, as shown in Table 2.5. The ratio of exchangeable <sup>137</sup>Cs from the two soil samples (E5 and E6) was less than 1 %, with 50–60 % of <sup>137</sup>Cs remaining in the residue. Approximately 98 % of <sup>137</sup>Cs was in the fraction of Fe–Mn oxide, organic matter, and the residue. The <sup>137</sup>Cs in the water fraction (F1) is undetectable and this is the same results of the extraction

**Table 2.4** Concentrations of  $^{137}\text{Cs}$  and  $^{134}\text{Cs}$  in surface soil collected in ETMA and Nagadoro

Sample No.	Depth	$^{134}\text{Cs}$	$^{137}\text{Cs}$	$^{134}\text{Cs}/^{137}\text{Cs}$
	cm	$\text{kBq}\cdot\text{m}^{-2\text{a}}$	$\text{kBq}\cdot\text{m}^{-2}$	Activity ratio
E5	0.0–2.5	$173 \pm 4$	$175 \pm 3$	$0.99 \pm 0.03$
	2.5–5.0	$0.911 \pm 0.059$	$0.722 \pm 0.041$	$1.26 \pm 0.11$
	5.0–10	$3.94 \pm 0.15$	$3.66 \pm 0.12$	$1.08 \pm 0.05$
Total	0.0–10	$178 \pm 1$	$179 \pm 1$	$0.99 \pm 0.01$
E6	0.0–2.5	$147 \pm 4$	$133 \pm 4$	$1.11 \pm 0.04$
	2.5–5.0	$22.7 \pm 0.8$	$20.3 \pm 0.6$	$1.12 \pm 0.05$
	5.0–10	$12.0 \pm 1.0$	$16 \pm 1$	$0.75 \pm 0.08$
Total	0.0–10	$182 \pm 1$	$169 \pm 1$	$1.07 \pm 0.01$
N1	cm	$\text{MBq}\cdot\text{m}^{-2}$	$\text{MBq}\cdot\text{m}^{-2}$	Activity ratio
	0.0–1.0	$26.6 \pm 0.5$	$26.4 \pm 0.3$	$1.01 \pm 0.02$
	1.0–2.0	$17.3 \pm 0.4$	$17.1 \pm 0.2$	$1.01 \pm 0.03$
	2.0–3.0	$18.6 \pm 0.4$	$18.9 \pm 0.2$	$0.98 \pm 0.02$
	3.0–4.0	$5.50 \pm 0.16$	$5.73 \pm 0.10$	$0.98 \pm 0.03$
	4.0–5.0	$2.76 \pm 0.06$	$2.82 \pm 0.04$	$0.98 \pm 0.03$
	5.0–10	$1.44 \pm 0.05$	$1.48 \pm 0.03$	$0.97 \pm 0.04$
	10–15	ND	ND	–
	15–20	ND	ND	–
	20–25	ND	ND	–
25–29	ND	ND	–	
Total	0.0–29	$72.3 \pm 0.7$	$72.5 \pm 0.4$	$1.00 \pm 0.01$

<sup>a</sup>Correction on March 11, 2011

test obtained in Table 2.5. The small fraction of exchangeable  $^{137}\text{Cs}$  suggests that immediately after the  $^{137}\text{Cs}$  in rainwater dropping on the surface soil,  $^{137}\text{Cs}$  and  $^{134}\text{Cs}$  were strongly adsorbed onto the soil of the Kanto loam, and they were not readily leached into the soil water. The amount of  $^{129}\text{I}$  in fraction of F1 and F2 were 0.7–9.5 % and 1–3.8 %, respectively; therefore,  $^{131}\text{I}$  in unsaturated soil moved downward faster than  $^{137}\text{Cs}$ . More than 90 % of  $^{137}\text{Cs}$  was in the fraction of organic matter and the residue, while  $^{129}\text{I}$  was mainly fixed by Fe-Mn oxidation and organically bound.

The estimated  $^{137}\text{Cs}$  migration rate for the Nishiyama loam soil, which was obtained in situ at Nishiyama (Nagasaki), is  $1.0 \text{ mm}\cdot\text{y}^{-1}$  [13]. This is considerably less than the rainwater infiltration rate of  $2.5 \text{ m}\cdot\text{y}^{-1}$ . Furthermore,  $^{137}\text{Cs}$  was not detected in the groundwater of the Nishiyama area, suggesting that  $^{137}\text{Cs}$  has not yet migrated to the groundwater table [14]. We collected 4 L of shallow groundwater in the Kashiwa city in the ETMA on August 17, 2012. The groundwater was filtered through membrane filter with a pore size of 80, 3, and  $0.45 \mu\text{m}$ . The groundwater after the filtration was gradually reduced to 5 mL by a mantle heater. Both  $^{137}\text{Cs}$  and  $^{134}\text{Cs}$  were not detected in the shallow groundwater and the suspended matters collected from the filter (Table 2.7).

**Table 2.5** Extraction of cesium isotopes in soil by pure water and groundwater (in Bq)

Nuclides/media	Pure water	Pure water	Groundwater	Groundwater
Sampling site	W1	W6	W6	E5
<sup>134</sup> Cs	ND (0.17)	ND (0.02)	ND (0.02)	ND (0.02)
<sup>137</sup> Cs	ND (0.16)	ND (0.02)	ND (0.02)	ND (0.02)
<sup>131</sup> I	ND (0.19)	–	–	–
<sup>136</sup> Cs	ND (0.15)	–	–	–
<sup>132</sup> Te	ND (0.14)	–	–	–
Period of extraction	30 min	90 day	90 day	90 day
Sampling date of soil	March 29, 2011	Aug. 25, 2011	Aug. 25, 2011	Aug. 25, 2011
Measuring time	10,000 s	864,000 s	864,000 s	864,000 s
Nuclides/media	Pure water	Pure water	Pure water	Groundwater
Sampling site	E5	E6	N1	N1
<sup>134</sup> Cs	ND (0.02)	ND (0.02)	ND (0.02)	ND (0.02)
<sup>137</sup> Cs	ND (0.02)	ND (0.02)	ND (0.02)	ND (0.02)
Period of extraction	270 day	270 day	90 day	270 day
Sampling date of soil	August 25, 2011	August 25, 2011	May 24, 2012	May 24, 2012
Measuring time	864,000 s	864,000 s	864,000 s	864,000 s

ND: below the detection limit, ( ): detection limit value

**Table 2.6** Distribution of <sup>137</sup>Cs and <sup>129</sup>I in the soil dissolved in each fraction solution

Fraction	E5 (%)	E6 (%)	N1 (%)
<sup>137</sup> Cs			
F1: Water	0.0	0.0	0.0
F2: Exchangeable	0.4	0.9	1.67
F3: Bound to carbonates	1.3	0.9	1.43
F4: Bound to Fe-Mn oxides	6.0	2.1	1.12
F5: Bound to organic matter	37.8	33.1	5.27
Residual	54.4	63.1	90.5
Total	100	100	100
<sup>129</sup> I			
F1: Water	9.5	0.8	0.74
F2: Exchangeable	3.8	1.0	2.40
F3: Bound to carbonates	5.4	1.3	3.92
F4: Bound to Fe-Mn oxides	72	20.9	82.3
F5: Bound to organic matter	9.2	66.4	0.91
Residual	–	9.6	9.74
Total	100	100	100

Although the <sup>131</sup>I moving velocity deduced from that of <sup>129</sup>I was greater than that of <sup>137</sup>Cs, the <sup>129</sup>I migration rate is lower than the water infiltration rate, due to the <sup>129</sup>I absorption on soil in the unsaturated zone.

In Kanto loam, soil water reaches depths of 20–30 cm, considering a 1–1.5 m·y<sup>-1</sup> infiltration rate, after 80 days corresponding to the time length of 10 times of the <sup>131</sup>I

**Table 2.7** Concentrations of  $^{137}\text{Cs}$  and  $^{134}\text{Cs}$  in groundwater and radioactivities of suspended matter (SS) of the groundwater sampled at the Tokyo metropolitan area after the accident

Nuclides	$^{131}\text{I}$ ( $\text{Bq}\cdot\text{kg}^{-1}$ )	$^{137}\text{Cs}$ ( $\text{Bq}\cdot\text{kg}^{-1}$ )	$^{134}\text{Cs}$ ( $\text{Bq}\cdot\text{kg}^{-1}$ )
Groundwater	ND (0.007)	ND (0.008)	ND (0.008)
SS ( $\sim 80\ \mu\text{m}$ )	ND	ND	ND
SS ( $80\ \mu\text{m} \sim 3\ \mu\text{m}$ )	ND	ND	ND
SS ( $3\ \mu\text{m} \sim 0.45\ \mu\text{m}$ )	ND	ND	ND

ND: below detection limit, ( ): detection limit value

half-lives. Mainly  $^{137}\text{Cs}$  was detected in litters in forest [5] but  $^{137}\text{Cs}$  was detected to depth of 10 cm in soil without litter [15]. Because rainy force is buffered in litters when the surface of soils has litters, rain is hard to directly enter to the deep part of the soil. Water-soluble  $^{131}\text{I}$  would merely move downward to depths of 30–40 cm, even if  $^{131}\text{I}$  penetrated a depth of 10 cm in the soil without litters and/or grass immediately after the accident. Therefore,  $^{131}\text{I}$  could never reach the depths of 50 cm in the groundwater table.

## 2.4 Conclusion

The sequentially chemical fractionations of  $^{129}\text{I}$  and  $^{137}\text{Cs}$  in soil indicate that most part of  $^{137}\text{Cs}$  and  $^{129}\text{I}$  were insoluble. Traces of  $^{131}\text{I}$  in the soil water did not reach the 50-cm depth by late June, 2011, corresponding to the time length of 10 times of  $^{131}\text{I}$  half-lives after the Fukushima NPP accident. Therefore, shallow groundwater could be safely useful water resource after the accident.

**Acknowledgment** This study is partially supported by JST Initiatives for Atomic Energy Basic and Generic Strategic Research. We are deeply appreciative of Dr. Iimoto for scientific support and advice for the groundwater sampling.

**Open Access** This chapter is distributed under the terms of the Creative Commons Attribution Noncommercial License, which permits any noncommercial use, distribution, and reproduction in any medium, provided the original author(s) and source are credited.

## References

1. Amano H, Akiyama M, Chunlei B, Kishimoto T, Kuroda T, Muroi T, Odaira T, Ohta Y, Takeda K, Watanabe Y, Morimoto T (2012) *J Environ Radioact* 111:42–52
2. Hirose K (2012) *J Environ Radioact* 111:13–17
3. Ohta T, Mahara Y, Kubota T, Fukutani S, Fujiwara K, Takamiya K, Yosinaga H, Mizuochi H, Igarashi T (2012) *J Environ Radioact* 111:38–41
4. Ohta T, Mahara Y, Kubota T, Igarashi T (2013) *Ana Sci* 29:941–947

5. Mahara Y, Ohta T, Ogawa H, Kumata A (2014) *Sci Rep* 4:Article number 7121. doi:[10.1038/srep07121](https://doi.org/10.1038/srep07121)
6. Muramatsu Y, Matsuzaki H, Toyama C, Ohno T (2015) *J Environ Radioact* 139:344–350
7. Miyake Y, Matsuzaki H, Fujiwara H, Saito T, Yamagata H, Honda M, Muramatsu Y (2012) *Geochem J* 46:327
8. Oughton DH, Salbu B, Riise G, Lien HN, Østby GA, Nøren A (1992) *Analyst* 117:481–486
9. Riise G, Bjørnstad HE, Lien HN, Oughton DH, Salbu B (1990) *J Radioanal Nucl Chem* 142:531–538
10. Ohta T, Mahara Y, Kubota T, Abe T, Matsueda H, Tokunaga T, Sekimoto S, Takamiya K, Fukutani S, Matsuzaki H (2013) *Nucl Instrum Methods Phys Res B* 294:559–562
11. Matsuzaki H, Muramatsu Y, Kato K, Yasumoto M, Nakano C (2007) *Nucl Instrum Methods Phys Res B* 259:721–726
12. Ohno T, Muramatsu Y, Miura Y, Oda K, Inagawa N, Ogawa H, Yamazaki A, Toyama C, Saito M (2012) *Geochem J* 46:287–295
13. Mahara Y (1993) *J Environ Qual* 22:722–730
14. Mahara Y, Miyahara S (1984) *J Geophys Res* 89:7931–7936
15. Multidisciplinary investigation on radiocesium fate and transport for safety assessment for interim storage and disposal of heterogeneous waste. The initiatives for atomic energy basic and generic strategic Research, JST, 2013, 240407 (in Japanese). Initiatives for Atomic Energy Basic and Generic Strategic Research by the Ministry of Education, Culture, Sports, Science and Technology of Japan

# Chapter 3

## Isotopic Ratio of $^{135}\text{Cs}/^{137}\text{Cs}$ in Fukushima Environmental Samples Collected in 2011

Takumi Kubota, Yuji Shibahara, Tomoko Ohta, Satoshi Fukutani, Toshiyuki Fujii, Koichi Takamiya, Satoshi Mizuno, and Hajimu Yamana

**Abstract** The isotopic ratios of radioactive cesium derived from the Fukushima accident were determined by  $\gamma$ -spectrometry and thermal ionization mass spectrometry (TIMS). In order to ascertain the initial ratios at the time of the accident, environmental samples collected during 2011 were used for the analysis. Soil, litter, and seaweed were incinerated, and the cesium contained therein was adsorbed into ammonium phosphomolybdate powder. The cesium in the seawater was adsorbed into AMP-PAN resin (Eichrom Technologies, LLC); its recovery ratio was almost one without the carrier being added. Incinerated samples and the AMP-PAN resin were then measured by  $\gamma$ -spectrometry. The cesium solution recovered from adsorbers was subjected to TIMS measurements. The isotopic ratios of  $^{134}\text{Cs}/^{137}\text{Cs}$  and  $^{135}\text{Cs}/^{137}\text{Cs}$  were found to be independent of the type of sample in question, as well as the sampling location; the ratios were 0.07 and 0.36 (decay correction: 11 March 2011), respectively, which differ from the results of atmospheric nuclear tests (i.e., 0 and 2.7, respectively). This difference in the ratio of  $^{135}\text{Cs}/^{137}\text{Cs}$  will contribute to estimations of the origin of radioactive contamination in the future.

**Keywords** Thermal ionization mass spectrometry • Fukushima accident • Environmental samples • Isotopic ratio of  $^{135}\text{Cs}/^{137}\text{Cs}$  and  $^{134}\text{Cs}/^{137}\text{Cs}$

### 3.1 Introduction

The Fukushima Daiichi Nuclear Power Plant (FDNPP) disaster gave rise to the release of a large amount of radioactive material into the environment [1–3]. Radioactive cesium nuclides were spread and stored in east Japan because of

---

T. Kubota (✉) • Y. Shibahara • S. Fukutani • T. Fujii • K. Takamiya • H. Yamana  
Research Reactor Institute, Kyoto University, Kumatori, Osaka 590-0494, Japan  
e-mail: [t\\_kubota@rri.kyoto-u.ac.jp](mailto:t_kubota@rri.kyoto-u.ac.jp)

T. Ohta  
Hokkaido University, Sapporo, Hokkaido 060-8628, Japan

S. Mizuno  
Nuclear Power Safety Division, Fukushima Prefectural Government, Fukushima 960-8043, Japan

their high volatility and long half-life. However, global fallout from atmospheric nuclear tests was the main contaminant source before the Fukushima accident [4]. Yellow sand, which flies from China in the spring, is known to contain radioactivity from atmospheric nuclear tests [5]. In addition to this periodic input, it is possible that radioactive contaminants from the Fukushima accident may be present. Even though the radioactive materials are found somewhere in the future, the environment can be considered to be the same situation before the Fukushima accident as long as they originate from the global fallout; in other words, the environment is not contaminated by the Fukushima accident. The migration of contaminants from the Fukushima accident is an important factor in resolving the Fukushima accident. It is natural that radioactive materials will be found even in locations far from Fukushima, such as west Japan, because of the global fallout. It is therefore important, from the perspective of future studies on Fukushima, to determine whether such contaminants originate from the Fukushima accident or not.

The use of nuclear energy, both in terms of nuclear reactors and nuclear weapons, provides several radioactive cesium nuclides in its products. The different production history in the two processes, however, results in different isotopic ratios of cesium.  $^{134}\text{Cs}$  is produced as a result of neutron irradiation of  $^{133}\text{Cs}$ , which can originate as a fission product. On the other hand, the production amount of  $^{134}\text{Cs}$  in nuclear tests can be ignored because nuclear reactions and neutron irradiation cease after an extremely short period of time. Accordingly,  $^{134}\text{Cs}$  is considered to be contaminant in nuclear reactors. Although  $^{135}\text{Cs}$  and  $^{137}\text{Cs}$  are produced as direct fission products, the production of  $^{135}\text{Cs}$  is affected by neutron irradiation conditions. Because  $^{135}\text{Xe}$ , which is the parent nuclide of  $^{135}\text{Cs}$ , has a large neutron capture cross section, the production of  $^{135}\text{Cs}$  is suppressed in long periods of neutron irradiation; this results in the isotopic ratio of  $^{135}\text{Cs}/^{137}\text{Cs}$  from nuclear reactors being different from that of nuclear tests. In this way, the isotopic ratios of Cs (e.g.,  $^{134}\text{Cs}/^{137}\text{Cs}$  and  $^{135}\text{Cs}/^{137}\text{Cs}$ ) can reveal the origin of contaminants in the environment.

Isotopic ratios can be determined in two ways:  $\gamma$ -spectrometry and mass spectrometry. It is easy to measure  $^{134}\text{Cs}$  and  $^{137}\text{Cs}$  by  $\gamma$ -spectrometry, a nondestructive analysis method. However, the  $^{135}\text{Cs}$  of pure beta emitter cannot be measured, and the decay of  $^{134}\text{Cs}$  (with a relatively short half-life) prohibits the isotopic analysis. On the other hand, mass spectrometry can determine the presence of  $^{134}\text{Cs}$ ,  $^{135}\text{Cs}$ , and  $^{137}\text{Cs}$  nuclides after chemical and/or physical purification. The measurement of  $^{135}\text{Cs}$  permits isotopic analysis even after the  $^{134}\text{Cs}$  has decayed out. Mass spectrometry can potentially be hindered by isobar nuclides; however, thermal ionization mass spectrometry (TIMS) with a high signal-to-noise ratio sufficiently suppresses the isobar effect. In the ionization process, isobar nuclides (in this study, cesium and barium) are separated according to their different ionization energies. We investigated various environmental samples by using TIMS [6], which is suitable for determining the isotopic ratios of radioactive cesium in the environment for long periods of time.

The isotopic ratio of  $^{135}\text{Cs}/^{137}\text{Cs}$  determined by TIMS can estimate the origin of contamination in environmental samples; this process requires the ratio at the time



of Fukushima accident to be used as the initial value. The initial values in various samples – not only soil and litter but also seawater and seaweed – are important factors in discussing the migration and mixing of radioactive cesium released in the Fukushima accident, other accidental releases, and atmospheric nuclear tests. In this study, the isotopic measurement of the various samples collected from May to September 2011 was conducted by  $\gamma$ -spectrometry and TIMS.

## 3.2 Materials and Methods

The environmental samples were collected in Fukushima prefecture from May to September 2011, and four of them were subjected to analysis. A litter sample was collected along Route 399 in Iitate village, where severe contamination was observed. Seawater and seaweed samples were collected at the Matsushita beach in Iwaki city. A soil sample was collected in Hinoemata village, which is one of the Fukushima local government's sampling plots.

Before analyzing the specific activity and isotopic ratios of cesium, the samples collected were treated as follows. The soil sample was dried at 105 °C and sieved through a 2 mm screen in order to remove pebbles, tree roots, and leaves; it was then incinerated at 450 °C in order to disintegrate organic matter. The litter sample was dried, cleaned by hand, and then incinerated. The seaweed sample was dried and incinerated without cleaning. An aliquot of these incinerated samples was dissolved in  $\text{HNO}_3$  and then purified with ammonium phosphomolybdate (AMP) [6] in order to recover the cesium fraction. The seawater sample was treated with AMP-PAN in order to concentrate the cesium, which was eluted with  $\text{NH}_4\text{OH}$ .

The radioactivity of  $^{134}\text{Cs}$  and  $^{137}\text{Cs}$  in incinerated samples and AMP-PAN was measured by  $\gamma$ -spectrometry. The radioactivity was measured with a HPGe semiconductor detector, which was calibrated with a standard radioactive source of  $^{137}\text{Cs}$  (662 keV) and  $^{60}\text{Co}$  (1132 and 1337 keV) [7]. Each sample was placed apart from the detector, thereby reducing the coincidence summing effect in the determination of  $^{134}\text{Cs}$ . In this case, the lower detection limit would rise; however, the radioactivity in samples was sufficiently high and could therefore be determined in this study. The isotopic ratios of  $^{134}\text{Cs}/^{137}\text{Cs}$  and  $^{135}\text{Cs}/^{137}\text{Cs}$  in the purified cesium fraction were measured by TIMS. The isotopic ratios of  $^{134}\text{Cs}/^{137}\text{Cs}$  and  $^{135}\text{Cs}/^{137}\text{Cs}$  were determined by TIMS, and a TaO activator was used to enhance the counting efficiency. The effect of isobaric barium can be ignored owing to the fact that it has a different ionization energy than cesium does [6].

## 3.3 Results and Discussion

In the analysis of radioactive cesium nuclides in seawater by  $\gamma$ -spectrometry, the natural cesium carrier is ordinarily added into the recovery process of cesium because of its low concentration. The addition of the carrier in mass spectrometry

**Table 3.1** Specific activity of  $^{137}\text{Cs}$  in AMP-PAN resin and the  $^{137}\text{Cs}$  recovery ratio

	Weight (g)	Radioactivity of $^{137}\text{Cs}$ (Bq)	Specific activity (Bq/kg)	Recovery ratio
1st column	0.87	$16.4 \pm 0.2$		
2nd column	1.49	$12.8 \pm 0.2$		
Total (15 kg seawater)		$29.2 \pm 0.3$	$1.95 \pm 0.02$	$0.97 \pm 0.10$
Initial [7]			$2.0 \pm 0.2$	

**Table 3.2** Radioactivity of  $^{134}\text{Cs}$  and  $^{137}\text{Cs}$  as determined by  $\gamma$ -spectrometry

Sample	Dry weight (g)	Radioactivity		Radioactivity ratio of $^{134}\text{Cs}/^{137}\text{Cs}$	Collection date	Location
		$^{134}\text{Cs}$ (Bq)	$^{137}\text{Cs}$ (Bq)			
Soil	12.98	$3.4 \pm 0.3$	$4.0 \pm 0.1$	$0.87 \pm 0.07$	15 September 2011	Hinoemata
Litter	15.90	$6562 \pm 57$	$6194 \pm 43$	$1.06 \pm 0.01$	23 May 2011	Iitate
Seaweed	17.78	$10.4 \pm 0.5$	$10.7 \pm 0.2$	$0.97 \pm 0.05$	25 August 2011	Iwaki
Seawater	AMP-PAN	$28.9 \pm 0.9$	$29.2 \pm 0.3$	$0.99 \pm 0.03$	25 August 2011	Iwaki

could prevent to detection of the signal isotopes of interest by isotope dilution, thereby decreasing isotopic ratios below detection limit and covering with large signal from the carrier added. A seawater sample of known concentration was used in order to confirm qualitative recovery without adding the carrier. The seawater sample was treated with  $\text{HNO}_3$  to pH 1 and then passed through two columns, connected in series and filled with AMP-PAN, at a rate of 5 kg/d. The specific activity of  $^{137}\text{Cs}$  and the recovery ratio onto the AMP-PAN resin, listed in Table 3.1, show that an AMP-PAN resin of about 2.5 g is sufficient for completely extracting cesium isotopes from 15 kg of seawater.

The specific activity in environmental samples (as determined by  $\gamma$ -spectrometry) and the activity ratio of  $^{134}\text{Cs}/^{137}\text{Cs}$  are listed in Table 3.2. The specific activity depends on the type of sample in question and the distance of the collection point from the FDNPP. However, the activity ratio shows that the contamination was derived from the Fukushima accident, although the activity ratio for soil collected at Hinoemata village is slightly low. The activity ratios were converted to isotopic ratios, which were then compared to the results of TIMS (see below).

The results of TIMS measurements are listed in Table 3.3, where the isotopic ratios evaluated from the results of  $\gamma$ -spectrometry are also listed. Among the four samples – litter, soil, seaweed, and seawater – only the litter sample yielded isotopic ratios for both  $^{134}\text{Cs}/^{137}\text{Cs}$  and  $^{135}\text{Cs}/^{137}\text{Cs}$ . In particular, the intensity of the signal from the soil sample was too low to evaluate both isotopic ratios. Other elements obviously interfered with the mass spectrometry measurements of the seaweed sample, and thus neither isotopic ratio was evaluated. Both evaluation failures were probably caused by inadequate processes and/or the shortcomings of the purification

**Table 3.3** Isotopic ratio of  $^{134}\text{Cs}/^{137}\text{Cs}$  and  $^{135}\text{Cs}/^{137}\text{Cs}$  as determined by  $\gamma$ -spectrometry and thermal ionization mass spectrometry (TIMS)

Sample	Isotopic ratio of $^{134}\text{Cs}/^{137}\text{Cs}$		Isotopic ratio of $^{135}\text{Cs}/^{137}\text{Cs}$	Distance from FDNPP	Reference	
	$\gamma$ -spectrometry	TIMS				
Soil	$0.059 \pm 0.005$	Not detected	Not detected	WSW, 160 km	This work	
Litter	$0.073 \pm 0.001$	$0.0691 \pm 0.0014$	$0.3574 \pm 0.0020$	NW, 34 km		
Seaweed	$0.067 \pm 0.003$	Not evaluated	Not evaluated	SSW, 55 km		
Seawater	$0.068 \pm 0.003$	Not evaluated	$0.3617 \pm 0.0051$	SSW, 55 km		
Grass	$0.069 \pm 0.009$	$0.0722 \pm 0.0004$	$0.3622 \pm 0.0006$	NW, 42 km		[6]
Bark	$0.067 \pm 0.002$	$0.0698 \pm 0.0005$	$0.3663 \pm 0.0005$	NNW, 3 km		
Root	$0.069 \pm 0.001$	$0.0684 \pm 0.0008$	$0.3586 \pm 0.0008$	WNW, 8 km		
Moss	$0.070 \pm 0.000$	$0.0713 \pm 0.0003$	$0.3663 \pm 0.0007$	SSW, 2 km		

process, which first requires the purification of cesium. The mass spectrometry of the seawater sample shows that the  $^{134}\text{Cs}$  signal overlapped with the tail of the  $^{133}\text{Cs}$  signal (see Fig. 3.1); nevertheless, the isotopic ratio of  $^{135}\text{Cs}/^{137}\text{Cs}$  can be obtained. Despite the fact that it is based on only one result of the litter sample, the isotopic ratio of  $^{134}\text{Cs}/^{137}\text{Cs}$  evaluated from TIMS is in good agreement with that from  $\gamma$ -spectrometry, thereby demonstrating the validity of both measurement methods. The isotopic ratios of  $^{135}\text{Cs}/^{137}\text{Cs}$  of the litter and the seawater sample collected in 2011 were both 0.36 (decay correction: 11 March 2011).

The results obtained in this study are now compared to those of other references. Those of the previous work [6] are listed in Table 3.3. The isotopic ratio of  $^{134}\text{Cs}/^{137}\text{Cs}$  in the samples (evaluated from both  $\gamma$ -spectrometry and TIMS) agrees with the results of the other study; however, the ratio of soil from Hinoemata is slightly lower. Furthermore, the isotopic ratios of  $^{135}\text{Cs}/^{137}\text{Cs}$  in land samples are in good agreement with that in the seawater sample, which did not yield an isotopic ratio for  $^{134}\text{Cs}/^{137}\text{Cs}$ . In another study [8], the isotopic ratios of  $^{135}\text{Cs}/^{137}\text{Cs}$  in litter, lichen, and soil samples were determined with inductively coupled plasma tandem mass spectrometry (ICP-MS/MS) to be 0.333–0.375, depending on location and distance from the FDNPP. These three studies showed that the environmental samples (both land and marine samples) collected from the area remarkably contaminated by the Fukushima accident had isotopic ratios of  $^{134}\text{Cs}/^{137}\text{Cs}$  of 0.07 and  $^{135}\text{Cs}/^{137}\text{Cs}$  of 0.36, which are quite different from the values that arise from global fallout; such values were mainly the result of atmospheric nuclear tests and were almost 0 and about 2.7, respectively [6]. The radioactivity of  $^{134}\text{Cs}$  will decrease to 1/30 of its initial value 10 y after the Fukushima accident, which will lead to difficulties in detecting  $^{134}\text{Cs}$ . However,  $^{135}\text{Cs}$  and  $^{137}\text{Cs}$  can be sufficiently detected by TIMS at that time, and thus the isotopic ratio of  $^{135}\text{Cs}/^{137}\text{Cs}$  related to the Fukushima accident and global fallout will become 0.44 and 3.4, respectively. The value of the isotopic ratio in environmental samples collected in the future can therefore demonstrate the origin of radioactive cesium by TIMS.

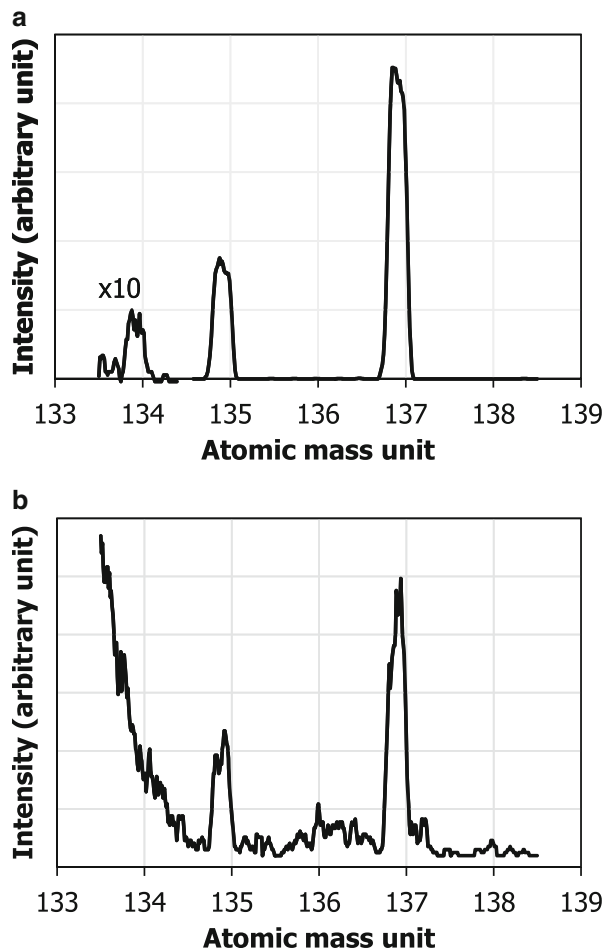


**Fig. 3.1** Mass spectrometry measurements obtained by thermal ionization mass spectrometry (TIMS) for (a) litter and (b) sea water

### 3.4 Conclusion

In order to obtain the initial isotopic ratios of cesium at the time of the Fukushima accident, environmental samples were collected in Fukushima prefecture during 2011. The samples were treated with AMP and AMP-PAN in order to purify and recover the cesium; using the latter technique, the cesium contained in seawater was almost completely recovered. The isotopic ratios of cesium were determined by  $\gamma$ -spectrometry and TIMS. These results were in good agreement with each other (i.e., the results were independent of the determination method used) and with other studies as well. However, further development in the purification of the

seaweed sample is required. On the basis of the initial isotopic ratio derived from the Fukushima accident, the isotopic ratio of cesium in environmental samples collected in the future can be expected to estimate the contribution of the accident through comparisons with the effects of global fallout.

**Acknowledgements** We wish to thank Mr. Mitsuyuki Konno and Mr. Satoru Matsuzaki for their help in collecting environmental samples and the Matsushimaya Ryokan staff for their support. This work was supported by the KUR Research Program for Scientific Basis of Nuclear Safety.

**Open Access** This chapter is distributed under the terms of the Creative Commons Attribution Noncommercial License, which permits any noncommercial use, distribution, and reproduction in any medium, provided the original author(s) and source are credited.

## References

1. Hirose K (2012) 2011 Fukushima Dai-ichi nuclear power plant accident: summary of regional radioactive deposition monitoring results. *J Environ Radioact* 111:13–17
2. Ohta T et al (2012) Prediction of groundwater contamination with  $^{137}\text{Cs}$  and  $^{131}\text{I}$  from the Fukushima nuclear accident in the Kanto district. *J Environ Radioact* 111:38–41
3. Tagami K et al (2011) Specific activity and activity ratios of radionuclides in soil collected about 20 km from the Fukushima Daiichi Nuclear Power Plant: radionuclide release to the south and southwest. *Sci Total Environ* 409:4885–4888
4. Hirose K et al (2008) Analysis of the 50-year records of the atmospheric deposition of long-lived radionuclides in Japan. *App Radiat Isot* 66:1675–1678
5. Fukuyama T et al (2008) Contribution of Asian dust to atmospheric deposition of radioactive cesium ( $^{137}\text{Cs}$ ). *Sci Total Environ* 405:389–395
6. Shibahara Y et al (2014) Analysis of cesium isotope compositions in environmental samples by thermal ionization mass spectrometry – 1. A preliminary study for source analysis of radioactive contamination in Fukushima prefecture. *J Nucl Sci Technol* 51:575–579
7. Kubota T et al (2013) Removal of radioactive cesium, strontium, and iodine from natural waters using bentonite, zeolite, and activated carbon. *J Radioanal Nucl Chem* 296:981–984
8. Zheng J et al (2014)  $^{135}\text{Cs}/^{137}\text{Cs}$  isotopic ratio as a new tracer of radiocesium released from the Fukushima nuclear accident. *Environ Sci Tech* 48:5433–5438

## Chapter 4

# Application of Mass Spectrometry for Analysis of Cesium and Strontium in Environmental Samples Obtained in Fukushima Prefecture

## Analysis of Cesium Isotope Compositions in Environmental Samples by Thermal Ionization Mass Spectrometry-2

Yuji Shibahara, Takumi Kubota, Satoshi Fukutani, Toshiyuki Fujii, Koichi Takamiya, Tomoko Ohta, Tomoyuki Shibata, Masako Yoshikawa, Mitsuyuki Konno, Satoshi Mizuno, and Hajimu Yamana

**Abstract** For the assessment of Fukushima Daiichi Nuclear Power Plant accident, the applicability of the thermal ionization mass spectrometry (TIMS), which is a type of mass spectrometry, was studied. For the study of the recovery/analysis method of cesium and strontium, at first, the radioactive cesium and strontium were generated by the irradiation of natural uranium at KUR. After this study, the applicability of this method to the environmental samples obtained in Fukushima prefecture was verified.

**Keywords** Fukushima Dai-ichi Nuclear Power Plant accident • Strontium • Cesium • Chromatography • Mass spectrometry • Isotopic ratio

---

Y. Shibahara (✉) • T. Kubota • S. Fukutani • T. Fujii • K. Takamiya • H. Yamana  
Kyoto University Research Reactor Institute, 2, Asashiro-Nishi, Kumatori-cho, Sennan,  
Osaka 590-0494, Japan  
e-mail: [y-shibahara@rri.kyoto-u.ac.jp](mailto:y-shibahara@rri.kyoto-u.ac.jp)

T. Ohta  
Hokkaido University, Kita 8, Nishi 5, Kita-ku, Sapporo, Hokkaido 060-8628, Japan

T. Shibata • M. Yoshikawa  
Kyoto University Institute for Geothermal Sciences, Noguchi-baru, Beppu, Oita 874-0903, Japan

M. Konno • S. Mizuno  
Nuclear Power Safety Division, Fukushima Prefectural Government, 8-2 Nakamachi, Fukushima,  
Fukushima 960-8043, Japan

## 4.1 Introduction

On the accident of Fukushima Daiichi Nuclear Power Plant (FDNPP), fission products (FP) such as radioactive Cs and Sr were widely released. The amounts of FP generated in each reactor were calculated by using ORIGEN code [1]. Many studies of radioactive Cs and Sr were performed to estimate external and internal exposures and to analyze the source of radioactive nuclides. These studies were typically performed by  $\gamma$ -ray spectrometry of  $^{134}\text{Cs}$  ( $T_{1/2} = 2.06$  y) and  $^{137}\text{Cs}$  ( $T_{1/2} = 30.2$  y) for the analysis of radioactive Cs and by  $\beta$ -spectrometry of  $^{90}\text{Sr}$  ( $T_{1/2} = 28.9$  y) for that of radioactive Sr.

In addition to  $^{134}\text{Cs}$  and  $^{137}\text{Cs}$ , radioactive  $^{135}\text{Cs}$  ( $T_{1/2} = 2.3 \times 10^6$ ) is also generated during the operation of reactors. Because of the difference in the generation process and the half-life of radioactive Cs, the isotopic ratios of  $^{134}\text{Cs}/^{137}\text{Cs}$  and  $^{135}\text{Cs}/^{137}\text{Cs}$  have been used for analyzing the operations of nuclear facilities [2–6]. Naturally occurring Sr has four stable isotopes ( $^{84}\text{Sr}$ ,  $^{86}\text{Sr}$ ,  $^{87}\text{Sr}$ , and  $^{88}\text{Sr}$ ), on the other hand, and the isotopic composition of Sr generated in reactors [1] are totally different from the natural abundance [7]. From the analysis data of the isotopic compositions, thus, the information on the origin of radioactive nuclide release would be obtained. The mass spectrometry provides the isotopic compositions of elements. Although mass spectrometry has been used for the analysis of radioactive nuclides and actinides, few studies have reported the analysis of radioactive Cs and Sr.

The purpose of the present study is to analyze Cs and Sr isotopes in environmental samples in Fukushima prefecture for source analysis and safety assessment. Although the amounts of radioactive Cs and Sr released in this accident were very huge, the contaminated environmental samples show the small radioactivity per unit weight of the contaminated environmental samples, since the contaminated area is very wide. For the study of the recovery/analysis method of cesium and strontium, at first, the radioactive Cs and Sr were generated by the irradiation of natural uranium at KUR. After this study, the applicability of this method to the environmental samples obtained in Fukushima prefecture was verified.

## 4.2 Experimental

### 4.2.1 Irradiation of $\text{UO}_2$ for Study of Radioactive Cs and Sr

10 mg of  $\text{UO}_2$  of natural uranium was irradiated for 3 h at the Kyoto University Research Reactor with the neutron flux  $5.5 \times 10^{12}$  n/s  $\text{cm}^2$ . From the calculation with ORIGEN-II code [8], the amounts of the major radionuclide of Cs and Sr were estimated as  $7.4 \times 10^{-11}$  g ( $^{137}\text{Cs}$ ) and  $4.5 \times 10^{-11}$  g ( $^{90}\text{Sr}$ ), respectively. After standing for *ca.* 2 days, radioactive Cs and Sr were recovered and analyzed.

## 4.2.2 Recovery of Cs and Sr

### 4.2.2.1 Isolation of TRU Elements

Cs and Sr were recovered with UTEVA<sup>TM</sup>-resin (100–150  $\mu\text{m}$ , Eichrom Technologies), Sr-resin (100–150  $\mu\text{m}$ , Eichrom Technologies), ammonium phosphomolybdate (AMP), the cation exchange resin DOWEX<sup>TM</sup> 50WX8 (100–200 mesh), and the anion exchange resin DOWEX<sup>TM</sup> 1 X 8 (100–200 mesh).

The irradiated  $\text{UO}_2$  was dissolved in 8 M  $\text{HNO}_3$  (TAMAPURE-AA-100) and was evaporated to dryness at 403 K. 8 M  $\text{HNO}_3$  was added and the insoluble residues removed by centrifugation. After centrifugation,  $\text{H}_2\text{O}_2$  (TAMAPURE-AA 100) was added for the preparation of 8 M  $\text{HNO}_3/0.3\%$   $\text{H}_2\text{O}_2$  sample solution to isolate TRU elements such as U and Pu by the extraction chromatography with UTEVA-resin [9].

Three milliliter of the UTEVA-resin conditioned with diluted nitric acid was filled into a column of 54 mm in length and 6.5 mm in diameter and pretreated with 10 mL of 8 M  $\text{HNO}_3/0.3\%$   $\text{H}_2\text{O}_2$  before loading the solution. After loading the solution, the UTEVA-resin was rinsed with 8 M  $\text{HNO}_3$  to elute alkaline earth metal elements [10]. The effluent was evaporated to dryness and dissolved in 10 mL of 3 M  $\text{HNO}_3$  solution for the extraction chromatography with Sr-resin.

### 4.2.2.2 Recovery of Strontium

The solution was loaded to the Sr-resin conditioned with diluted nitric acid and filled into a column of 54 mm in length and 6.5 mm in diameter up to 3 mL. This effluent was evaporated at 403 K and the residue dissolved in 0.05 M  $\text{HNO}_3$  for the recovery of Cs. After washing of the Sr-resin with 3 M  $\text{HNO}_3$ , Sr was recovered with 20 mL of 0.05 M  $\text{HNO}_3$ , evaporated to dryness, and dissolved in 10  $\mu\text{L}$  of 1 M  $\text{HNO}_3$ .

### 4.2.2.3 Recovery of Cesium

After adding of 0.1 g of AMP to the Cs solution and stirring for several hours, the supernatant was removed from the mixed solution by centrifugation. A 20 mL 3 M ammonium hydroxide (TAMAPURE-AA 100) solution was used to dissolve the residue for subsequent anion-exchange ion chromatography.

After the final conditioning [11], a 3 mL portion of the anion-exchange resin was added to a column of 54 mm in length and 6.5 mm in diameter. The sample solution was added to the column, and the resulting eluate was collected and heated to dryness. The residue was dissolved in 20 mL of 0.1 M  $\text{HNO}_3$  for the final purification with the cation-exchange ion chromatography.



The cation-exchange resin conditioned with hydrofluoric acid (TAMAPURE-AA-100), etc. [12] was filled into a column of 42 mm in length and 5.0 mm in diameter up to 1.5 mL. After loading the sample solution, the resin was washed with diluted nitric acid followed by 20 mL of 1.5 M HCl (TAMAPURE-AA 100) to recover Cs. The effluent was heated to dryness, and the residue was dissolved in 20  $\mu\text{L}$  of 1 M  $\text{HNO}_3$  for the analysis of the isotopic composition of Cs.

### ***4.2.3 Analysis of Isotopic Composition of Cesium and Strontium***

Isotopic compositions of Cs and Sr were measured with a TIMS (Triton-T1, Thermo Fisher Scientific). A 1  $\mu\text{L}$  aliquot of each solution was loaded onto a rhenium filament with a TaO activator [13]. The standard material of SRM987 [14] was used as a reference material of mass spectrometry of Sr. The mass spectra of radioactive Cs and Sr were obtained with a secondary electron multiplier detector (SEM) because of the low total amounts of radionuclide loaded onto the filament.

### ***4.2.4 Analysis of Environmental Samples***

The plant samples were obtained from the south area of Iitate village, the northeast area of Okuma town, the southeast area of Futaba town, and southwest area of Futaba town in Fukushima prefecture from November 2012 and May 2013 (Table 4.1). The samples were washed three times with pure water and dried at 373 K. About 2.5 g of the dried samples was incinerated with a ring furnace at 873 K and dissolved in concentrated  $\text{HNO}_3$  at 403 K and evaporated to dryness. 20 mL of 8  $\text{HNO}_3$  was added and the insoluble residues removed by centrifugation for the preparation of recovery of Cs and Sr. Recovery of Cs and Sr from environmental samples was also carried out by the same manner described above.

The concentration of  $^{88}\text{Sr}$  was measured with an inductively coupled quadrupole mass spectrometer (ICP-QMS, HP-4500, Yokoagawa) and radioactivity of  $^{90}\text{Sr}$  by Cherenkov counting [15]. The total concentration of radioactive Cs was measured by  $\gamma$ -spectrometry. The sample solutions were prepared as 50 ppm of  $^{88}\text{Sr}$  in 1 M  $\text{HNO}_3$  for the analysis of Sr and 5000 Bq/mL for  $^{137}\text{Cs}$  in 1 M  $\text{HNO}_3$  for the analysis of Cs. The mass spectra of radioactive Cs and Sr were obtained with a SEM, while those of stable Cs and Sr were obtained with Faraday cup detector, since the amounts of stable nuclide were much larger than those of radionuclide.

**Table 4.1** List of samples and results of  $^{87}\text{Sr}/^{86}\text{Sr}$  isotopic ratio measurement

Sampling area	Sample ID	Type	$\delta_{87/86}^a$	Remarks
Iitate village (37.61 N, 140.80E)	ITT01	Grass ( <i>Artemisia indica</i> )	-3.28(01)	ITT01 to 07 were prepared by division of one sample
	ITT02		-3.04(04)	
	ITT03		-3.20(09)	
	ITT04		-3.05(07)	
	ITT05		-3.11(07)	
	ITT06		-3.13(08)	
	ITT07 <sup>b</sup>		-3.14(04)	
		ITT-av	-3.14(06)	
Okuma town (37.41 N, 141.03E)	OKM01 <sup>b</sup>	Moss	-1.42(12)	
	OKM02 <sup>c</sup>	Moss	-1.83(05)	
	OKM03	Bark ( <i>Metasequoia glyp- tostroboides</i> )	-4.42(08)	
Futaba town-1 (37.45 N, 141.62E)	FTB01 <sup>b</sup>	Bark ( <i>Cryptomeria japonica</i> )	-2.51(08)	
	FTB02	Leaves of tree ( <i>Camellia japonica</i> )	-3.75(09)	
	FTB03	Leaves of tree	-3.87(15)	Same tree ( <i>Cryptomeria japonica</i> ), 03: attached leaves; 04: fallen leaves
	FTB04	Leaves of tree	-4.14(09)	
	FTB05	Grass ( <i>Artemisia indica</i> )	-3.29(09)	
	FTB06		-4.23(08)	
Futaba town-2 (37.45 N, 140.94E)	FTB35R <sup>b</sup>	Grass( <i>Artemisia indica</i> )	-2.96(08)	Same grass, 35R: roots; 35 L: leaves
	FTB35L		-4.30(08)	
Austria	IAEA-156	Grass ( <i>Clover</i> )	-2.27(03)	

<sup>a</sup>Parentheses means experimental error in  $\pm 2$  s.d

<sup>b</sup>Isotopic ratio of radioactive Cs has been reported in our previous study [11]

<sup>c</sup>Isotopic ratio of radioactive Cs was analyzed in this study

## 4.3 Results and Discussion

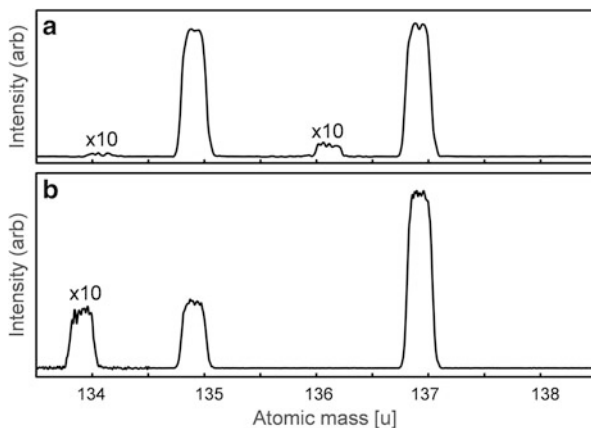
### 4.3.1 Isotopic Analysis of Radioactive Cs and Sr from Irradiated $\text{UO}_2$

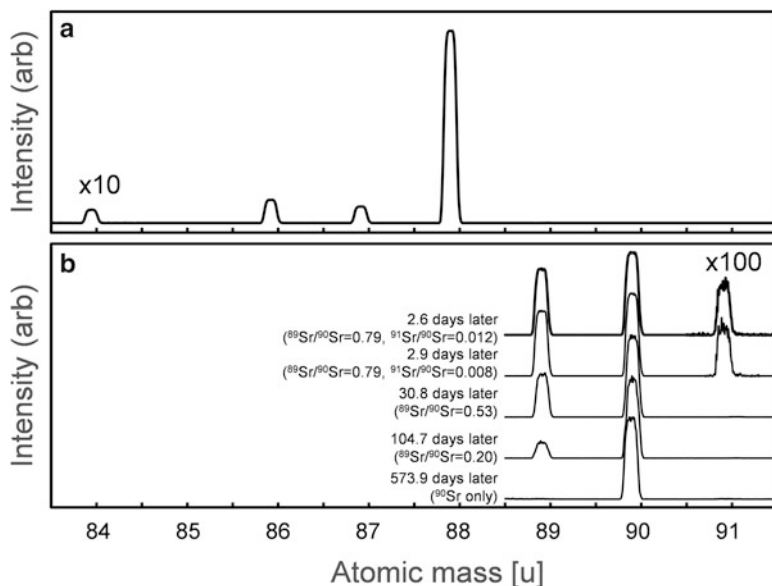
Figure 4.1a shows the mass spectra of Cs recovered from the irradiated  $\text{UO}_2$ . In this measurement,  $^{135}\text{Cs}$ ,  $^{136}\text{Cs}$ , and  $^{137}\text{Cs}$  were detected:  $^{134}\text{Cs}$  was not detected, because of the difference in the generation scheme. The observed isotopic ratios of  $^{135}\text{Cs}/^{137}\text{Cs}$  and  $^{136}\text{Cs}/^{137}\text{Cs}$  were obtained as  $0.9103 \pm 0.0008$  and  $0.00022 \pm 0.00001$ . From our calculation with ORIGEN-II code [8], the loading amounts of  $^{135}\text{Cs}$ ,  $^{136}\text{Cs}$ , and  $^{137}\text{Cs}$  in this time were about 3.5, 0.03, and 3.7 pg respectively. This means that the femtogram level of Cs is detectable by TIMS.

Figure 4.2 shows the mass spectra of Sr both of stable (a) and radioactive (b) isotopes. At the measurement of 2.6 days later,  $^{89}\text{Sr}$ ,  $^{90}\text{Sr}$ , and  $^{91}\text{Sr}$  were detected. From our calculation with ORIGEN-II code [8], the loading amounts of  $^{89}\text{Sr}$ ,  $^{90}\text{Sr}$ , and  $^{91}\text{Sr}$  in this time were about 3, 4, and 0.04 pg respectively. This means that the femtogram level of Sr is also detectable by TIMS.

The measured isotopic ratios were 0.80 for  $^{89}\text{Sr}/^{90}\text{Sr}$  and 0.01 for  $^{91}\text{Sr}/^{90}\text{Sr}$  showing the agreement with the calculated value (0.79 for  $^{89}\text{Sr}/^{90}\text{Sr}$  and 0.01 for  $^{91}\text{Sr}/^{90}\text{Sr}$ ). Because the half-life of  $^{91}\text{Sr}$  is 9.5 h, the mass spectrum of  $^{91}\text{Sr}$  disappeared at the measurement of 31 days later. The measured isotopic ratio of  $^{89}\text{Sr}/^{90}\text{Sr}$  is 0.53 showing the agreement with the calculated value of 0.54. At the measurement of 574 days later, only the mass spectrum of  $^{90}\text{Sr}$  was observed because the half-life of  $^{89}\text{Sr}$  is 50.5 days. This means that  $^{89}\text{Sr}/^{90}\text{Sr}$  could not be analyzed by using a typical mass spectrometer after Sep. 2012, if we obtain the sample containing femtogram level of  $^{90}\text{Sr}$ . The isotopic ratio of  $^{90}\text{Sr}/^{\text{stable}}\text{Sr}$  would be therefore needed for our purpose.

**Fig. 4.1** Mass spectra of Cs. (a) Recovered from  $\text{UO}_2$  irradiated in KUR. (b) Recovered from environmental sample from Fukushima prefecture (Reproduced from Ref [11])





**Fig. 4.2** Mass spectra of Sr. Stable isotopes (a) were obtained by measurement of Sr of SRM987 with a Faraday cup detector, and radioactive isotopes (b) were obtained by measurement of Sr recovered from UO<sub>2</sub> irradiated in KUR with a secondary electron multiplier detector

### 4.3.2 Analysis of Isotopic Compositions of Cs and Sr from Environmental Samples

#### 4.3.2.1 Analysis of Cs

Figure 4.1b shows three peaks, representing <sup>134</sup>Cs, <sup>135</sup>Cs, and <sup>137</sup>Cs, were observed on the typical mass spectra of Cs recovered from environmental samples obtained in Fukushima prefecture [11], while the peak representing <sup>136</sup>Cs was not observed because of the half-life ( $T_{1/2} = 13.2$  d). From the calculation with ORIGEN-II code [1], the isotopic ratio of <sup>136</sup>Cs/<sup>137</sup>Cs in the fuel was estimated as *ca.* 0.00032. This value shows the same order compared with that of the irradiated UO<sub>2</sub>, suggesting that we could obtain the three isotopic ratios of <sup>134</sup>Cs/<sup>137</sup>Cs, <sup>135</sup>Cs/<sup>137</sup>Cs, and <sup>136</sup>Cs/<sup>137</sup>Cs until July 2011. Since there are three reactors in FDNPP, three isotopic ratios would bring the important information for the source analysis of radioactive Cs in the contaminated area in Fukushima prefecture.

Although we could not obtain the isotopic ratio of <sup>136</sup>Cs/<sup>137</sup>Cs after July 2011, we can obtain the two-dimensional map with the isotopic ratios of <sup>134</sup>Cs/<sup>137</sup>Cs and <sup>135</sup>Cs/<sup>137</sup>Cs as shown in Fig. 4.3. All of the isotopic ratios of <sup>135</sup>Cs/<sup>137</sup>Cs showed less than 0.4. This value was also much smaller than reported isotopic ratios of global fallout ( $\sim 0.5$  for Chernobyl accident and  $\sim 2.7$  for nuclear weapon testing, corrected

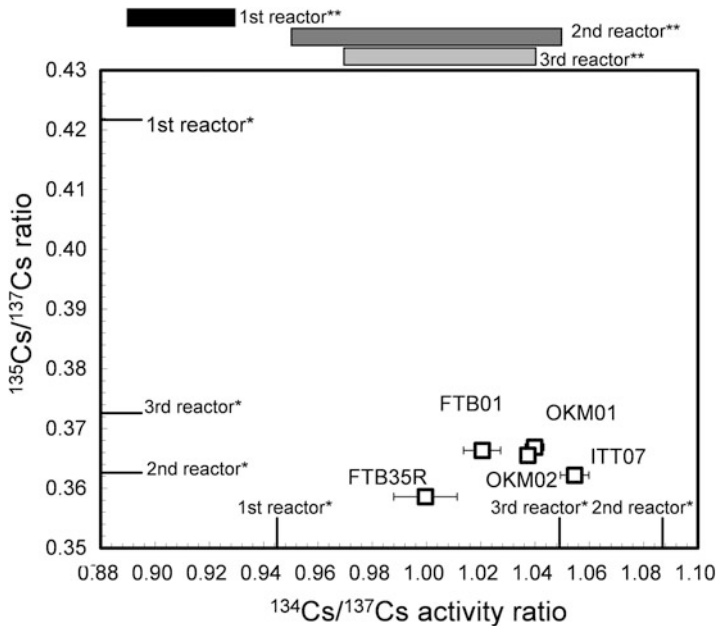


**Fig. 4.3**  $^{135}\text{Cs}/^{137}\text{Cs}$  (atomic ratio) vs  $^{134}\text{Cs}/^{137}\text{Cs}$  (activity ratio). Error here means  $\pm 2\text{SE}$ . Data of OKM01, FTB01, FTB35R and ITT07 were reproduced from Ref [11]. Both of isotopic ratio was corrected to March 11, 2011. Single asterisk (\*) represents calculation results from estimation of radioactive nuclides with ORIGEN-II code [1]. Double asterisk (\*\*) represents values reported for  $^{134}\text{Cs}/^{137}\text{Cs}$  activity ratio in polluted water [22]

to March 11, 2011 [11]) and the long half-life of  $^{135}\text{Cs}$  ( $T_{1/2} = 2.3 \times 10^6$  y), meaning that only the isotopic ratio of  $^{135}\text{Cs}/^{137}\text{Cs}$  would also provide the information for the origin of radioactive Cs among Chernobyl accident, nuclear weapon testing, and FDNPP accident for the long term.

#### 4.3.2.2 Analysis of Sr

The FP of Sr in each reactor has mainly five isotopes [1]: two stable isotopes of  $^{86}\text{Sr}$  and  $^{88}\text{Sr}$  and three radioactive isotopes of  $^{89}\text{Sr}$ ,  $^{90}\text{Sr}$ , and  $^{91}\text{Sr}$ . The relationship between the isotopic ratio of radioactive Cs and that of Sr estimated by ORIGEN Code calculation [1] is plotted in Fig. 4.4. In addition to the radioactive isotopes, the stable isotopes of Sr generated in each reactor show the characteristic profile. This suggests that the stable isotopes of Sr could be also used for the analysis of the FP of Sr.

Among the isotopic ratios of stable isotopes, the isotopic ratio of  $^{87}\text{Sr}/^{86}\text{Sr}$  is important in the field of the geological chronology [16], because  $^{87}\text{Sr}$  is generated by the  $\beta$ -decay of  $^{87}\text{Rb}$  having the half-life of  $4.9 \times 10^{10}$  y. Thus, the isotopic ratio of stable isotopes, in this study, will be focused on the isotopic ratio of  $^{87}\text{Sr}/^{86}\text{Sr}$ .

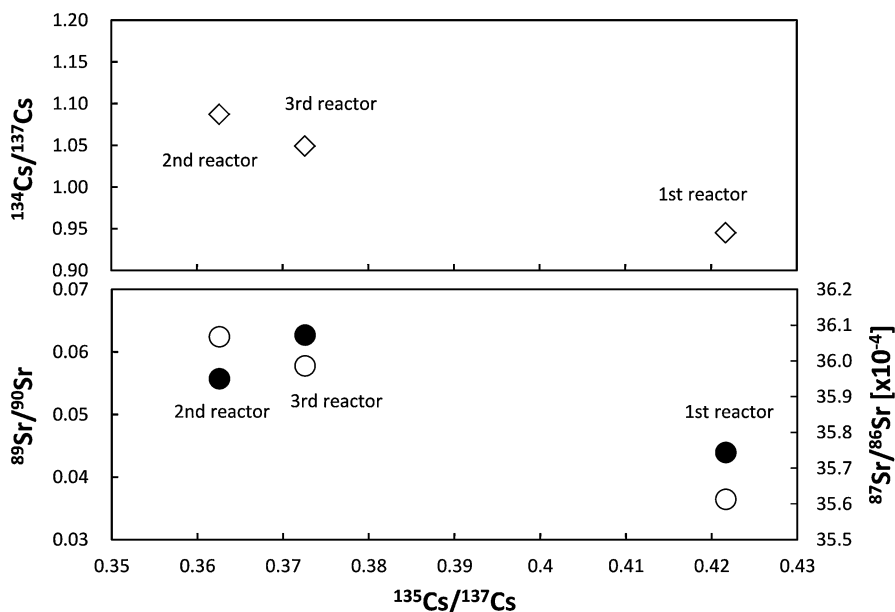


**Fig. 4.4** Estimated relationship between isotopic ratios of  $^{134}\text{Cs}/^{137}\text{Cs}$ ,  $^{89}\text{Sr}/^{90}\text{Sr}$  and  $^{87}\text{Sr}/^{86}\text{Sr}$  and that of  $^{135}\text{Cs}/^{137}\text{Cs}$ . Isotopic ratios were estimated by calculation results with ORIGEN Code [1]. *Open circle* means isotopic ratio of  $^{89}\text{Sr}/^{90}\text{Sr}$ . *Closed circle* represents isotopic ratio of  $^{87}\text{Sr}/^{86}\text{Sr}$

The certified value for SRM987 of the isotopic ratio of  $^{87}\text{Sr}/^{86}\text{Sr}$  showing the 95 % confidence intervals is  $0.71036 \pm 0.00026$  [14]. The averaged measurement value was obtained as  $0.71025 \pm 0.00002$  ( $n = 26$ ) showing the agreement with the certified value.

In this study, the variations in the isotopic ratio of  $^{87}\text{Sr}/^{86}\text{Sr}$  were normalized with that of SRM987; this would be expressed as delta-value ( $\delta_{87/86}$ ) in per mill notation as the following equation:

$$\delta_{87/86} = \left( \frac{(^{87}\text{Sr}/^{86}\text{Sr})_{\text{sample}}}{(^{87}\text{Sr}/^{86}\text{Sr})_{\text{SRM987}}} \right) \times 1000.$$

The samples of ITT01 to ITT07 were prepared by the division of one sample. The  $\delta_{87/86}$ -values of samples ITT01 to ITT07 in Table 4.1 agreed within the error showing the reproducibility of the isotopic ratio measurement including chemical treatment. From the  $\delta_{87/86}$ -values of samples ITT01 to ITT07, the averaged  $\delta_{87/86}$ -value of them was obtained to be  $\delta_{87/86} = -3.14 \pm 0.06$  ‰.

The results of the isotopic ratio measurements for all samples are summarized in Table 4.1 and shown in Fig. 4.5a. The result of the measurement for the reference material of IAEA-156: Radionuclides in clover [17] is also included. This reference material contains *ca.* 0.0075 Bq/g in June 2015. The  $\delta_{87/86}$ -values of the samples of

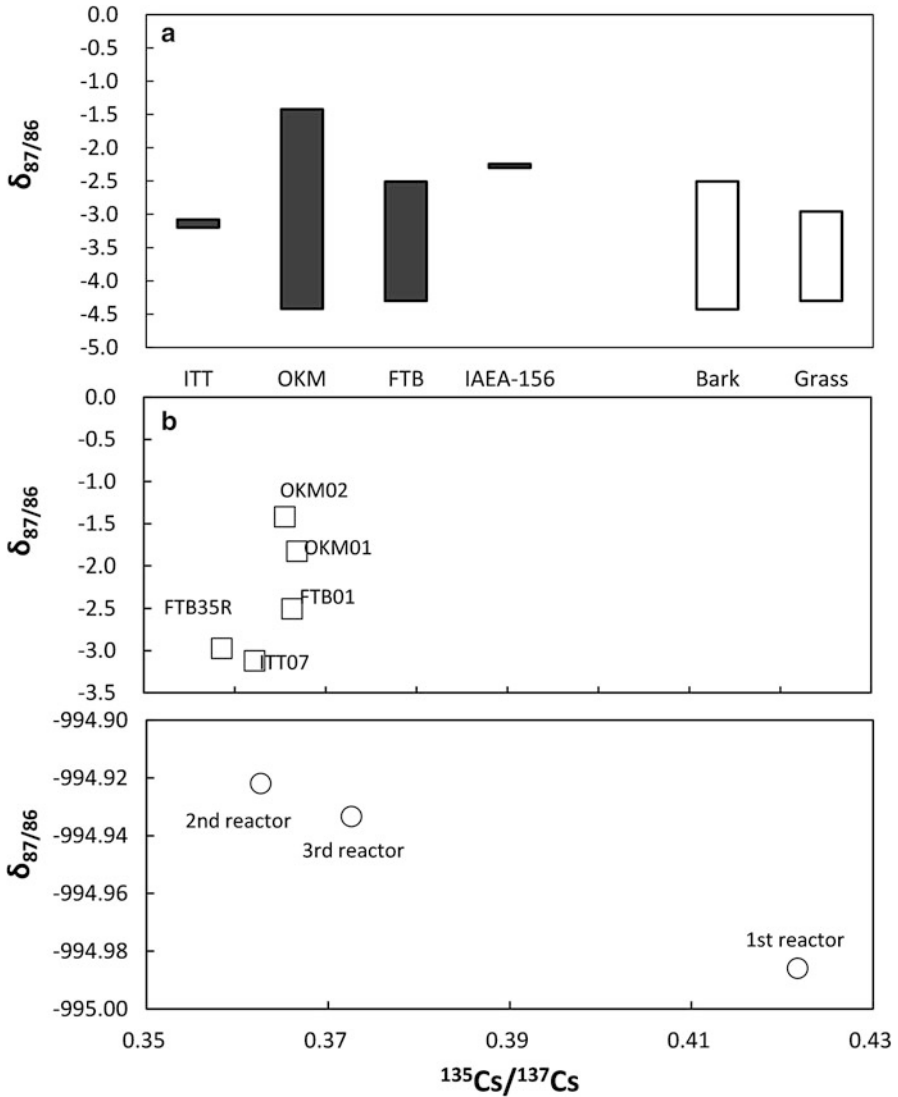


**Fig. 4.5** Results of  $^{87}\text{Sr}/^{86}\text{Sr}$  isotopic ratio measurement for plant samples (a), and isotopic ratio of  $^{87}\text{Sr}/^{86}\text{Sr}$  as a function of  $^{135}\text{Cs}/^{137}\text{Cs}$  (b). Bark is results of comparison between OKM03 and FTB01. Grass shows results of comparison between FTB35R and FTB35L. Isotopic ratio of  $^{135}\text{Cs}/^{137}\text{Cs}$  of OKM01, FTB01, FTB35R and ITT07 were reproduced from Ref [11], and used after time correlation on March 11, 2011. *Open square* and *open circle* mean analytical results in this study and results of estimation by calculation results with ORIGEN Code [1]

Okuma range from  $-1.4$  to  $-4.4$ , while those of Futaba range from  $-2.5$  to  $-4.2$ . It is found that these values have significant difference, by comparison with the  $\delta_{87/86}$ -value of Iitate samples.

Though the samples OKM03 and FTB01 are bark samples from the plants of the same family, these showed different magnitudes (Fig. 4.5a and Table 4.1). The isotopic ratio of  $^{87}\text{Sr}/^{86}\text{Sr}$  has received attention as the indicator of the production region of plants and reported the  $\delta_{87/86}$ -values ranged from  $-25.0$  to  $5.5$  [18]. As the reason of the difference in the  $\delta_{87/86}$ -values among samples OKM03 and FTB01, two origins could be considered: the first is the difference in the  $\delta_{87/86}$ -values of soils of sampling point (as the supply source of Sr) and the second is the difference in the degree of the isotope fractionation during the translocation process (considered as the reason of the difference in the isotopic ratio between the parts of the identical organism). Because of the comparison of the  $\delta_{87/86}$ -values of the same parts in this case, the difference in the  $\delta_{87/86}$ -value among samples OKM03 and FTB01 might be caused by the soils in sampling area.

If the difference of  $\delta_{87/86}$ -values between samples OKM03 and FTB01 originated from a difference of contamination level by the FP of Sr, the isotopic ratio may show a correlation as

$$\begin{aligned} \left( \frac{[^{87}\text{Sr}]_{\text{OKM03}}}{[^{86}\text{Sr}]_{\text{OKM03}}} \right) &= \left( \frac{[^{87}\text{Sr}]_{\text{nat}}}{[^{86}\text{Sr}]_{\text{nat}}} \right) \times (1 - X) \\ &\quad + \left( \frac{[^{87}\text{Sr}]_{\text{FP}}}{[^{86}\text{Sr}]_{\text{FP}}} \right) \times X, \\ \left( \frac{[^{87}\text{Sr}]_{\text{FTB01}}}{[^{86}\text{Sr}]_{\text{FTB01}}} \right) &= \left( \frac{[^{87}\text{Sr}]_{\text{nat}}}{[^{86}\text{Sr}]_{\text{nat}}} \right) \times (1 - Y) \\ &\quad + \left( \frac{[^{87}\text{Sr}]_{\text{FP}}}{[^{86}\text{Sr}]_{\text{FP}}} \right) \times Y. \end{aligned}$$

According to the relation and the concentrations of Sr; 72 ppm for OKM03 and 24 ppm for FTB03, the amount of the FP of  $^{86}\text{Sr}$  contained in the sample OKM03 would be higher than that of FTB01, about 10.3 ng. This is equivalent to *ca.* 10.5  $\mu\text{g}$  of  $^{90}\text{Sr}$  (*ca.*  $5.3 \times 10^7$  Bq) according to the averaged isotopic ratio of  $^{90}\text{Sr}/^{86}\text{Sr}$  of the FP of Sr [1].  $^{90}\text{Sr}$  was not found in the plant samples by TIMS and Cherenkov counting having the detection limit of several ten mBq/g [15], however, suggesting that our samples contain  $^{90}\text{Sr} < 10$  fg and was less than 1 Bq/g.

Sample FTB35R is roots, while FTB35L is leaves, of the same plant. The  $\delta_{87/86}$ -values (Fig. 4.5a and Table 4.1) showed a significant difference. Sample FTB35R shows higher  $\delta_{87/86}$ -value compared with sample FTB35L. The isotopic fractionations were observed in some biological processes. For example, the isotopic analysis of Sr [19], Fe [20], and Zn [21] proves that roots are isotopically heavy compared with the aerial parts; the maximum  $\delta_{87/86}$ -value was *ca.*  $-5.0$  for Sr, the maximum  $\delta_{56/54}$ -value was *ca.*  $-1.4$  for Fe, and the maximum  $\delta_{66/64}$ -value was *ca.*  $-0.26$  for Zn, respectively. Since the Cherenkov counting showed the amounts of  $^{90}\text{Sr}$  in these samples were under the detection limit, the difference in the  $\delta_{87/86}$ -value between samples FTB35R and FTB35L might be caused by the isotopic fractionations in the biological processes along with the contamination of sample FTB35R by the soil.



The isotopic ratios of radioactive Cs in samples FTB01, OKM01, FTB35R, and ITT07 measured by TIMS have been reported in our previous study [11], and that in OKM02 was measured in this study. The relationships between the isotopic ratio of  $^{87}\text{Sr}/^{86}\text{Sr}$  as  $\delta_{87/86}$ -value of these samples and that of  $^{135}\text{Cs}/^{137}\text{Cs}$  are plotted in Fig. 4.5b. The isotopic ratios of  $^{135}\text{Cs}/^{137}\text{Cs}$  show the significant difference from the reported values of the global fallout (*ca.* 0.5 for Chernobyl accident and *ca.* 2.7 for nuclear weapon testing corrected on March 11, 2011 [11]), while these values agreed with the estimated values with the results of ORIGEN Code calculation [1]. This means that all of the samples are contaminated by radioactive Cs released from FDNPP. The  $\delta_{87/86}$ -values of these samples, on the other hand, are far from that of the FP calculated by ORIGEN Code [1]. This suggests that the amount of deposit of  $^{90}\text{Sr}$  is very little compared with that of Cs and agrees with our previous report [15].

Although  $^{90}\text{Sr}$  was not found in the plant samples suggesting that our samples contain  $^{90}\text{Sr} < 10$  fg, typical mass spectrometers have the external analytical precision of ppm level. Assumed that this precision could be applied for the isotopic ratio of  $^{90}\text{Sr}/^{\text{stable}}\text{Sr}$ , the isotopic ratio of  $^{90}\text{Sr}/^{\text{stable}}\text{Sr}$  must be higher than  $10^{-6}$ . For the natural sample, since the Sr concentration ranges from ppb level to several hundred ppm level (Fig. 4.6), the detectable lower limit of the isotopic ratio of  $^{90}\text{Sr}/^{\text{stable}}\text{Sr}$  can be evaluated.

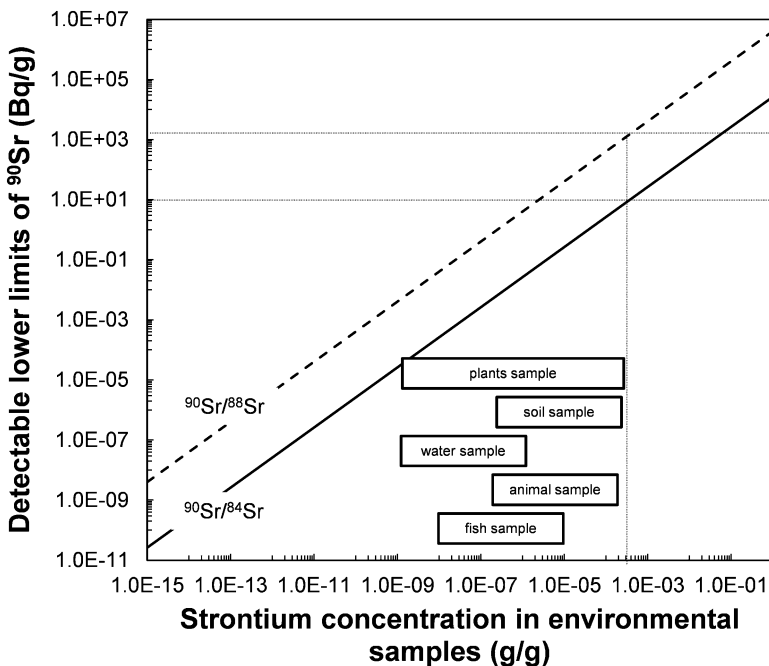


**Fig. 4.6** Detectable lower limits of  $^{90}\text{Sr}$  in environmental samples with TIMS. *Solid line* indicates a limit for  $^{90}\text{Sr}/^{84}\text{Sr}$ , and *broken line* a limit for  $^{90}\text{Sr}/^{88}\text{Sr}$

If  $^{88}\text{Sr}$  having the natural abundance *ca.* 82 % was used as reference isotope, the concentration of  $^{90}\text{Sr}$  should be higher than 1 Bq/g in almost any type of sample. When the isotopic ratio of  $^{90}\text{Sr}/^{84}\text{Sr}$  is used, because the abundance of  $^{84}\text{Sr}$  (*ca.* 0.56 %) is lower than that of  $^{88}\text{Sr}$ , the applicable range will become much wider than the case of  $^{88}\text{Sr}$  (Fig. 4.5). The improvement in the sensitivity of  $^{90}\text{Sr}$  detection and the obtaining of samples including small amounts of natural Sr will also bring wide applicable range.

## 4.4 Conclusions

Cs and Sr recovered from samples were analyzed by TIMS to study the applicability of TIMS for safety assessment and source analysis.

For the study of the recovery/analysis method of Cs and Sr, Cs and Sr were recovered from the natural uranium irradiated at KUR. From the measurement of radionuclide recovered from irradiated  $\text{UO}_2$ , it was concluded that several tens of femtogram level of radionuclide is detectable.

Cs and Sr were recovered from the environmental samples obtained from Fukushima prefecture and were analyzed by a method based on the results of irradiated  $\text{UO}_2$ . In the case of the analysis of Cs, it was confirmed that the analysis of the radioactive Cs by TIMS would provide important information for the source analysis. The isotopic ratio of  $^{135}\text{Cs}/^{137}\text{Cs}$  was useful for the precise evaluation of the radioactive Cs from FDNPP apart from that of global fallout after the radioactivity of  $^{134}\text{Cs}$  became below the detection limit of  $\gamma$ -ray measurement.

In the case of the analysis of Sr, on the other hand, the presence of  $^{90}\text{Sr}$  was not detected in any samples, while the changes in the isotopic ratios of  $^{87}\text{Sr}/^{86}\text{Sr}$  were observed. From the discussion for the amount of the FP of Sr, it was conjectured that the changes in the isotopic ratios of  $^{87}\text{Sr}/^{86}\text{Sr}$  might be brought by some isotopic fractionation in the biological processes. The evaluation of the detectable lower limit of the isotopic ratio of  $^{90}\text{Sr}/^{\text{stable}}\text{Sr}$  suggests that the isotopic ratio of  $^{90}\text{Sr}/^{84}\text{Sr}$  is the most suitable index to judge a source of radioactive Sr released during the accident of FDNPP by TIMS.

**Open Access** This chapter is distributed under the terms of the Creative Commons Attribution Noncommercial License, which permits any noncommercial use, distribution, and reproduction in any medium, provided the original author(s) and source are credited.

## References

1. Nishihara K, Iwamoto H, Suyama K (2012) JAEA-data/code 2012-018 [in Japanese]
2. Karam LR, Pibida L, McMahon CA (2002) Appl Rad Isot 56:369-374
3. Pibida L, MacMahon CA, Busharw BA (2004) Appl Rad Isot 60:567-570

4. Taylor VF, Evans RD, Cornett RJ (2008) *J Environ Radact* 99:109–118
5. Delmore JE, Snyder DC, Tranter T, Mann NR (2011) *J Environ Radact* 102:1008–1011
6. Snyder DC, Delmore JE, Tranter T, Mann NR, Abbott ML, Olson JE (2012) *J Environ Radact* 110:46–52
7. Berglund M, Wieser ME (2011) *Pure Appl Chem* 83:397–410
8. Ludwig SB, Renier JP (1989) Standard- and extended-Burnup PWR and BWR reactor models for the ORIGEN2 Computer Code. Oak Ridge National Laboratory, ORNL/TM-11018
9. Shibahara Y, Kubota T, Fujii T, Fukutani S, Ohta T, Takamiya K, Okumura R, Mizuno S, Yamana H (2015) *J Radioanal Nucl Chem* 303:1421–1424
10. Lee MH, Park JH, Oh SY, Ahn HJ, Lee CH, Song K, Lee MS (2011) *Talanta* 86:99–102
11. Shibahara Y, Kubota T, Fujii T, Fukutani S, Ohta T, Takamiya K, Okumura R, Mizuno S, Yamana H (2014) *J Nucl Sci Technol* 51:575–579
12. Yoshikawa M, Nakamura E (1993) *J Min Petr Econ Geol* 88:548–561
13. Birck JL (1986) *Chem Geol* 56:73–83
14. [https://www-s.nist.gov/srmors/view\\_detail.cfm?srm=987](https://www-s.nist.gov/srmors/view_detail.cfm?srm=987). Accessed 20 Aug 2014
15. Kubota T, Shibahara Y, Fujii T, Fukutani S, Ohta T, Takamiya K, Okumura R, Mizuno S, Yamana H (2015) *J Radioanal Nucl Chem* 303:39–46
16. Faure G, Powell JL (1972) *Strontium isotope geology*. Springer, New York
17. Strachnov V, Valkovic V, Dekner R (1991) Report on the intercomparison run IAEA-156: radionuclides in clover. International Atomic Energy Agency, Austria, IAEA/AL/035
18. Almeida CM, Vasconcelos MTSD (2001) *J Anal At Spectrom* 16:607–611
19. de Souza GF, Reynolds BC, Kiczka M, Bourdon B (2010) *Geochim Cosmochim Acta* 74:2596–2614
20. Moynier F, Fujii T, Wang K, Foriel J (2013) *Compt Rend Geosci* 345:230–240
21. Weiss DJ, Mason TFD, Zhao FJ, Kirk GJD, Coles BJ, Horstwood MSA (2005) *New Phytol* 165:703–710
22. Komori M, Shozugawa K, Nogawa N, Matsuo M (2013) *Bunseki Kagaku* 62:475–483 [in Japanese]

## Chapter 5

# Migration of Radioactive Cesium to Water from Grass and Fallen Leaves

Hirokuni Yamanishi, Masayo Inagaki, Genichiro Wakabayashi,  
Sin-ya Hohara, Tetsuo Itoh, and Michio Furukawa

**Abstract** The TEPCO Fukushima Daiichi Nuclear Power Plant accident in March 2011 led to high amounts of emitted radioactive Cs being deposited on land by both rainwater and snowfall. In addition, a significant amount of Cs was deposited on the surface of leaves, and after the accident, both trees and grasses absorbed radioactive Cs through their roots. In order to assess the effect on water sources, it is therefore important to evaluate the amount of radioactive Cs migrating to the water from both grass and fallen leaves.

A number of samples of clover, dandelion, and mugwort were collected from the Yamakiya elementary school in Kawamata-machi, Date-gun, Fukushima-ken in May 2013 and May 2014. Fallen leaves were also sampled from the wood adjoining the school. Measurement of the Cs content in water was carried out by placing the sample in water for over 400 days at 10–30 °C. The radioactive Cs content was measured using the HPGe detector. In the case of grass, the amount of migration to water was saturated after about 120 days. The saturation levels of migration rate to water varied with kinds of grass in the range of 0.2–0.8. The migration rate for fallen leaves was not larger than 0.13. In addition, after leaching from grass or fallen leaves into water, the absorption of radioactive Cs to soil was observed, and therefore, migration would be limited to a small area.

**Keywords** Fallen leaves • Grass • Migration • Radioactive cesium • Waste decontamination • Water

---

H. Yamanishi (✉) • M. Inagaki • G. Wakabayashi • S.-y. Hohara • T. Itoh  
Atomic Energy Research Institute, Kinki University, 3-4-1 Kowakae, Higashi-osaka,  
Osaka 577-8502, Japan  
e-mail: [yamanisi@kindai.ac.jp](mailto:yamanisi@kindai.ac.jp)

M. Furukawa  
Mayor of Kawamata-machi, Fukushima-ken, 30, Gohyakuda, Kawamata-machi, Date-gun,  
Fukushima-ken 960-1492, Japan

## 5.1 Introduction

A large amount of radioactive material was released by the nuclear power plant accident at the TEPCO Fukushima Daiichi site (1F site) in March 2011 [1]. The radioactive particles were transported by the prevailing wind and were deposited on the ground by both rain and snowfall. Due to these factors, the level of radiation in surrounding areas has been raised through the presence of radioactive material on the ground. As radiocesium is a source of both external exposure and internal exposure, its environmental behavior is of particular interest. Radiocesium adheres strongly to clays in the surface soil [2], and a very small amount is absorbed upon contact with water. Radiocesium was also deposited on the surface of leaves. In addition, following the deposition on the soil surface, trees and grasses absorbed the radiocesium in the soil through their roots.

Due to their long half-lives, Cs-134 (2 years) and Cs-137 (30 years) are responsible for the ongoing presence of radioactive materials outside the 1F site, even 4 years after the event. In the contaminated area outside the 1F site, decontamination work is now underway on residential land spaces and public facilities. During this process, the topsoil is removed and collected, and dried grass and fallen leaves are collected as contaminated waste. The waste for decontamination is stored in a flexible impermeable 1-m<sup>3</sup> bag and kept in a temporary depot for subsequent decontamination.

We are particularly interested in determining the quantity of radiocesium that migrates to water from grasses, fallen leaves, and soil. The environmental behavior of radiocesium was previously studied following the Chernobyl nuclear plant accident [3]. However, it is difficult to apply the result to Fukushima, as the environmental conditions such as soil type, precipitation amount, and temperature are very different at the two sites. The annual rainfall is approximately 1166 mm in Fukushima but only 621 mm in Pripyat, the town of Chernobyl. Due to the higher quantity of rainfall in Fukushima, it is possible that radiocesium is transferred through water. In addition, it should be considered that the chemical form of radiocesium that deposits in Fukushima is different to that deposited in Chernobyl. It is therefore necessary to use samples collected in Fukushima to study the environmental behavior of radiocesium in this area.

In order to assess the effect on water sources, it is therefore considered important to evaluate the amount of radiocesium migrating to the water from grass and fallen leaves. We herein report a process for the determination of the Cs content in grass and fallen leaves and in water following leaching. Samples collected in Fukushima will be used for the studies. We expect that it will be possible to use the obtained results for the prediction of radiocesium behavior in the environment.

## 5.2 Materials and Methods

### 5.2.1 *Sample Collection*

Environmental samples for this study were collected from the grounds of the Yamakiya elementary school, Kawamata-machi, Fukushima-ken, Japan. Fallen radiocesium gave a high topsoil Cs-137 content of 50 Bq/g in May 2011 [4]. Accuracy was expected to be improved using grass collected from the contamination site, rather than grass grown in a laboratory. In addition, at the contamination site, fallen leaves contained radiocesium on their surface due to deposition. Samples of clover, dandelion, pine needles, and mugwort were collected in May 2013 and May 2014. Fallen leaves were also collected in the forest that adjoins the school. In May 2013 and May 2014, the measured ambient dose rates at 1 m above ground level are 0.5–1.2 and 0.2–0.8  $\mu\text{Sv/h}$ , respectively.

Kawamata-machi is located approximately 40 km to the northwest of the 1F site. Following the accident, as the estimated annual dose was expected to exceed 20 mSv, the Yamakiya area in the southeast of Kawamata-machi was appointed a planned evacuation zone on April 22, 2011. The staff at the Atomic Energy Research Institute of Kinki University investigated the environmental radiation in cooperation with Kawamata-machi and began the collection of data, which contributed to understanding the radiation situation and aided in the discussions relating to the implementation of control measures [4, 5].

### 5.2.2 *Sample Preparation*

In order to prepare the plant samples for measurement, they were first preprocessed. First, the roots were removed from the grass samples, as they held soil that was contaminated with radiocesium. Other samples were washed with water to remove the soil particles on the surface of the samples. After washing, the samples were dried either in air or in an oven at 60 °C. The dried samples (15 g) were chopped finely (<1 cm length) and were placed into a U-8 container for measurement. The radiocesium concentration in each sample was measured using a hyperpure germanium semiconductor detector (HPGe detector).

### 5.2.3 *Radiocesium Migration to Water*

The measured samples (15 g) were divided into four equally sized portions and each portion placed into a water-permeable bag (95 × 70 mm), which was weaved with composite fiber composed of polyethylene, polypropylene, and polyester. The four bags containing the samples were soaked in water (500 mL) in a plastic

container ( $18 \times 13 \times 5$  cm), which was tightly closed, and allowed to stand for over 400 days. After this time, the resulting contaminated water was filtered, collected, and weighed. As the radiocesium concentrations in the sample were low, it was desirable to remove as much water as possible from the sample to precisely measure radioactivity. This was initially achieved by means of an evaporating dish and mantle heater. The dried matter was scraped away from the surface of the dish by washing with water (10 mL) and was moved to a U-8 container. The sample was then dried further by evaporation using an infrared oven. The radiocesium contents of samples were measured using the HPGe detector to give the radioactivity of the radiocesium that migrated to water from the plant samples.

Using the sample collected in May 2014, a similar experiment was conducted, which compares the migration rate to water using both deionized water and rainwater. The soaking period was 10–135 days, and the temperature was controlled at 25 °C.

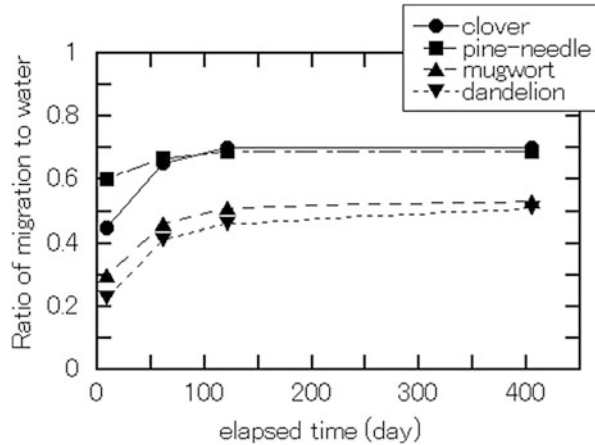
#### ***5.2.4 Radiocesium Deposition in Soil***

Radiocesium migrates to water from grass by means of soaking. However, water is often in contact with soil, and as the clay minerals present in soil strongly adsorb radiocesium, it is expected that the radiocesium in water can be deposited in soil. We therefore decided to investigate this by exposing soil to a solution containing radiocesium for 3 days, and the variations in radiocesium concentration in the solutions were measured. The solution required for this experiment was prepared using fallen leaves gathered at the Yamakiya Elementary School. Radiocesium was leached from the leaves by means of an ultrasound bath. The radiocesium concentration was then increased by reduction in the water content using an evaporating dish and a heating mantle. The radiocesium concentration in the solution was determined using an HPGe detector. A solution containing radiocesium (100 mL) was added to samples of dry field soil (10 or 30 g), and the resulting mixture was left to stand at 20–25 °C for either 14 h or 3 days. After this time, the aqueous solution was filtered to remove all soil particles and collected. The resulting residual radiocesium concentrations of all four solutions (10 g, 14 h), (30 g, 14 h), (10 g, 3 days), and (30 g, 3 days) were measured using an HPGe detector.

### **5.3 Results and Discussion**

We first examined the sample collected in May 2013. The radioactivities of Cs-137 in the dried sample (15 g) before soaking were calculated to be  $5.9 \pm 0.2$  Bq,  $2.6 \pm 0.2$  Bq,  $18.5 \pm 0.4$  Bq,  $3.0 \pm 0.1$  Bq,  $102 \pm 2$  Bq, and  $369 \pm 3$  Bq, for clover, pine needles, mugwort, dandelion, fallen leaves (broad leaf), and fallen leaves (needle leaf), respectively. The amounts of Cs-137 eluted from each sample

**Fig. 5.1** Change in migration rate from grass with the elapsed days



after soaking for 9 days were calculated to be  $2.7 \pm 0.1$  Bq,  $1.60 \pm 0.04$  Bq,  $5.5 \pm 0.2$  Bq,  $0.70 \pm 0.03$  Bq,  $8.2 \pm 0.2$  Bq, and  $6.3 \pm 0.2$  Bq, with an approximate 10-fold difference between the maximum and minimum values obtained. The migration rate is defined as the ratio of the radioactivity that migrated to water to the radioactivity of the sample before soaking. These migration rates were calculated to be  $0.45 \pm 0.03$ ,  $0.60 \pm 0.04$ ,  $0.30 \pm 0.01$ ,  $0.23 \pm 0.01$ ,  $0.08 \pm 0.002$ , and  $0.017 \pm 0.001$ . Fallen leaves have ratios in the range of 0.02–0.08 while grass exhibited larger ratios of 0.23–0.60.

After collection of the water, it was poured once more into the plastic container and was left to stand at 10–30 °C. This operation was repeated three times over different timeframes, more specifically, 50, 60, and 280 days, corresponding to 60, 120, and 400 days after beginning the soaking period, respectively. Figures 5.1 and 5.2 show the variation in migration rate over time. As shown in Fig. 5.1, in the case of grass, almost all the radiocesium which can be migrated had migrated to water after 60 days. In addition, it could be seen that after 120 days, little migration was observed, and so the total migration rate for 120 days was comparable to that for 400 days. In contrast, as shown in Fig. 5.2, the migration rate for fallen leaves was small, although an increase in migration rate even after 400 days was observed. This difference between grass and fallen leaves may be due to a number of reasons. Firstly, it must be considered that the radiocesium present in grass had been absorbed through the roots from the soil. This component of radiocesium might be present within the grass tissue due to weak adsorption, and thus may migrate to water. This would therefore result in a large migration rate for grass. In contrast, the radiocesium released following the accident was deposited on the surface of fallen leaves and was not absorbed through the roots. In addition, the radiocesium present on the fallen leaves did not migrate as easily to water, as the fallen leaves had been exposed to rain, and their surfaces washed before sampling. The migration rate shown in Fig. 5.2 is therefore small.



**Fig. 5.2** Change in migration rate from fallen leaves and soil with the elapsed days

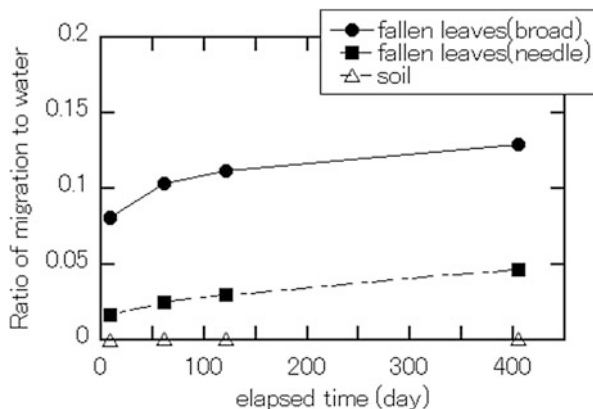
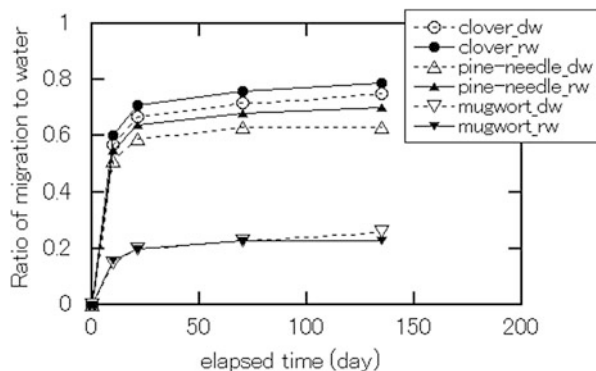


Figure 5.2 also shows the migration rate of radiocesium from dry soil (90 g) to water (500 mL). It was observed that the migration rate was very low. In addition, the migration rates increased over time, with a rate of  $(3.5 \pm 0.1) \times 10^{-4}$  recorded after 10 days and  $(1.2 \pm 0.1) \times 10^{-3}$  after 400 days.

Using the sample collected on May 2014, the migration rate for deionized water was compared with that obtained for rainwater. These samples were soaked in water for 10–135 days at 25 °C. As can be seen in Fig. 5.3, the differences between the two specifications of water were very small. Figures 5.4 and 5.5 show the variation in migration rate over time. The increasing trends of total migration have a similar pattern to Figs. 5.1 and 5.2. The migration rates from clover or pine needle were larger than that from mugwort, while the migration rate from fallen broad leaves was larger than that from fallen needle leaves.

Finally, Fig. 5.6 shows the results of the residual rate to solution (i.e., the ratio of concentration after soaking to concentration before soaking). The concentration of Cs-137 in the solution before the adsorption experiments was  $0.177 \pm 0.004$  Bq/g. The residual rate in the case of 10 g soil was  $0.29 \pm 0.02$  after soaking for 14 h and  $0.17 \pm 0.01$  after soaking for 3 days. The residual rate in the case of 30 g soil was calculated as  $0.11 \pm 0.01$  after soaking for 14 h and  $0.07 \pm 0.01$  after soaking for 3 days. These data demonstrate that the residual rate decreases according to both the quantity of soil and according to the number of days in the soaking period. This is likely due to the large quantities of soil present in the area, and thus the radiocesium could not be transported through a large area. This would also not be possible even through migration to water, as the radiocesium would be rapidly adsorbed into the soil.

**Fig. 5.3** Comparison of water, deionized water (dw) and rain water (rw)



**Fig. 5.4** Change in migration rate from grass with the elapsed days (using the sample May 2014)

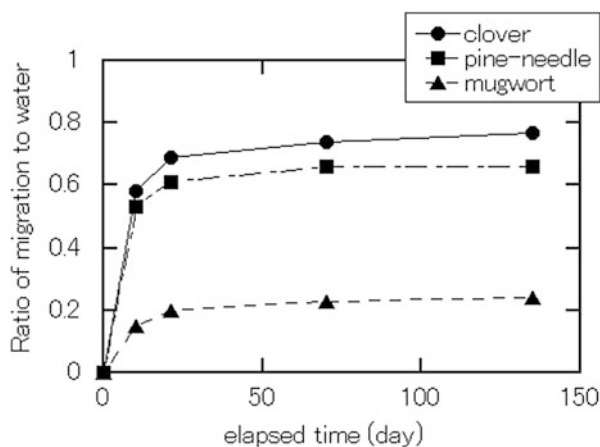


**Fig. 5.5** Change in migration rate from fallen leaves and soil with the elapsed days (using the sample May 2014)

